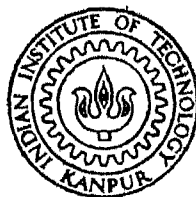# FREE VIBRATION OF THIN WALLED OPEN SECTION BEAMS WITH UNCONSTRAINED DAMPING LAYER

By

JITENDRA PRASAD VERMA

DEPARTMENT OF MECHANICAL ENGINEERING

INDIAN INSTITUTE OF TECHNOLOGY, KANPUR

SEPTEMBER, 1979

FREE VIBRATION OF THIN WALLED OPEN SECTION BEAMS WITH UNCONSTRAINED DAMPING LAYER

A Thesis Submitted
In Partial Fulfilment of the Requirements
for the Degree of
MASTER OF TECHNOLOGY

By

JITENDRA PRASAD VERMA

to the

DEPARTMENT OF MECHANICAL ENGINEERING
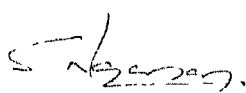
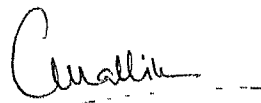INDIAN INSTITUTE OF TECHNOLOGY, KANPUR

SEPTEMBER, 1979

TH
620.3
V59f

ME-1979 - M-VER- FRE

CERTIFICATE

This is to certify that the thesis entitled "Free Vibration of Thin Walled Open Section Beams with Unconstrained Damping Layer" by J.P. Verma, is a record of the work carried out under our supervision and has not been submitted elsewhere for the award of degree.

S. Narayanan
Asstt. Professor
Department of Aero. Engg.
I.I.T. Kanpur

A.K. Mallik
Asstt. Professor
Department of Mech. Engg.
I.I.T. Kanpur

September 1979.

ACKNOWLEDGEMENT

CONTENTS

LIST OF FIGURES

LIST   OF   TABLES

NOMENCLATURE

A, A_1 — Area of cross-section of base material

A_2 — Area of cross-section of viscoelastic layer

C — Mass centre of the cross section with or without damping layer

C_1 — Torsional rigidity of the composite cross-section

C_2 — Warping rigidity of the composite cross-section

C_s — Saint Venant's torsional constant for original cross-section

C_w, C_{w_1} — Warping constants for the elastic layer

C_{w_2} — Warping constant for the viscoelastic layer

c_z — Distance between mass centre and shear centre

D — Shift of the composite neutral axis from that of the original beam cross section

$E., E_1$ — Young's modulus of elasticity of base material

E_2^* — Complex modulus of elasticity of viscoelastic material

E_2 — Real part of E_2^*

e — Distance of shear centre from the centre line of the upper horizontal portion of the cross section

F_1, F_2 — Forces on Elastic and Viscoelastic layers

G_1, G — Shear modulus of base material

G_2^* — Complex modulus of rigidity of viscoelastic material

h — Length of the vertical web of cross section

H_{21} — Distance between the neutral axes of two different layers

I_{η_1}, I_{η_2} — Area moments of inertia of the elastic and viscoelastic portions of beam about η axis passing through composite mass centre

I_{ζ_1}, I_{ζ_2} — Area moments of inertia of the two layers about ζ axis

$I_{\eta}, I_{\eta_{11}}$ — Area moment of inertia of the base cross-section about its own centroidal η axis

$I_{\eta_{22}}$ — Area moment of inertia of the added layer about its own centroidal η axis

I_{c_1}, I_{c_2} — Polar moment of inertia of the two layers about longitudinal axis

l — Length of the beam

l_1 — Lower Flange width of the cross section

l_2 — Length of the upper horizontal portion of the cross section

O — Shear centre of the cross section with or without damping layer

t_1 — Thickness of the elastic cross section

t_2 — Thickness of the viscoelastic layer

v_c, v_o — Deflection of C and O along Y direction

w — Displacement along Z direction.

w_d — Warping displacement

w_s — Warping function

$\bar{w}_s$ — Average warping function

X, Y, Z — Co-ordinate axes passing through shear centre

$\alpha_1, \alpha_2, \alpha_3, \alpha_4$ Nondimensional terms in characteristic polynomial equation

β — Loss factor of viscoelastic material

ε — Strain in the layers

η — Composite loss factor

λ_i — Roots of characteristic polynomial equation

χ, η, ζ — Coordinate axes passing through mass centre

ρ_1, ρ_2 — Mass density of the elastic and viscoelastic material

σ — Normal stresses in the layers

ψ — Rotation of cross-section about X axis

γ — Shear strain in layers

ω — Natural frequency

Ω_c^* — Complex nondimensional natural frequency in the coupled vibration of composite beam

Ω_c — Real part of Ω_c^*

Ω_n — Nondimensional natural frequency in coupled mode of vibration of the original cross-section

τ — Shear stresses in the layers

SYNOPSIS

of the

Dissertation on

FREE VIBRATION OF THIN WALLED OPEN
SECTION BEAMS WITH UNCONSTRAINED
DAMPING LAYER

Submitted in Partial Fulfilment of
the Requirement for the Degree

of

MASTER OF TECHNOLOGY

by

J.P. VERMA

DEPARTMENT OF MECHANICAL ENGINEERING
INDIAN INSTITUTE OF TECHNOLOGY, KANPUR

September 1979

        Free vibration characteristics of a thin walled
open cross section beam with unconstrained damping layer is
studied in the present work. A typical example of a top hat
section with viscoelastic layer at the flanges is considered.
Transverse vibrations both in and out of the plane (coupled
bending and twisting modes) of symmetry are investigated.
Results are obtained for natural frequencies and modal loss
factors in both these modes of vibration. Beams with simply
supported and clamped end conditions are investigated.
Extensive parametric investigations are carried out with an
efficient algorithm based on two dimension Newton-Raphson
technique.

CHAPTER 1

INTRODUCTION

1.1 Introduction

Control of vibration is an important aspect in the design of resonant systems. This is necessary in order to avoid early fatigue failure and malfunctioning of such systems. .Vibrations control is also of significance in view of human comfort especially in vehicular systems.

The level of vibration in a system can be reduced in a number of ways. These include, among others, (i) reduction of the excitation, (ii) isolation of the source, (iii) introduction of vibration neutralizers and (iv) detuning and decoupling by proper design. For resonant systems, however, increase in the damping is the most effective way of controlling excessive vibration. Several damping treatments have been devised and practiced towards this end. For example, damping tapes are applied to aircraft structures with a view to increase the fatigue life and reduce the interior. cabin noise. Mastic deadners serve the same purpose in automobiles.

The fuselage of an aircraft is subjected to convected random pressure field from the jet noise and turbulent boundary layer. As a result, the fuselage vibrates and in

turn radiates noise into the passenger cabin. Cabin noise in the mid and high frequency regions can be adequately attenuated by skin damping tape or fiberglass insulation. However, these methods are not very effective at low frequencies.

A concept similar to that of the tuned vibration damper has been attempted [1] in the design of the aircraft skin construction to reduce the vibration levels at low frequencies. This concept has been referred to as 'intrinsic tuning'. For a typical skin-stringer combination, the frequency of peak response is very close to the natural frequency of the individual skin bay (f_p), clamped along the stringers and simply supported along the frames. If stringer and panel dimensions are such that the natural frequency of the stringer (f_s) concides with f_p, then the stringer can act as a tuned absorber. To increase the effectiveness of the intrinsically tuned stringer over a broad frequency range, it is highly desirable to introduce additional damping. Additional damping in the stringer can be incorporated by various methods. The most common methods are

i) to have unconstrained or constrained visco-elastic layers on the stringer flanges,

ii) to use inherently high damping composites or alloys as the stringer material.

Stringers are thin walled open sections beam type structures. No adequate theory is available for the vibration analysis of such structures with layered damping

treatment. The purpose of the present thesis is to make a theoretical investigation of such problems.

1.2 Short Review of Previous Work

Work on layered damping treatments was initiated by Oberst and Lienard [2] . They considered the problem of an unconstrained layer damping treatment. The overall damping capacity of the composite plate was expressed in terms of the loss factor. Kerwin [3] investigated the problem of a constrained visco-elastic layer where loss modulus in shear contributes predominantly towards overall damping. Ross, Kerwin and Ungar [4] derived a general theory for free harmonic wave motions of an infinitely long beam made of three layers. An expression for the overall loss factor as a function of frequency was derived. The theory was valid only for simply supported end conditions in the case of finite beams. Ditaranto [5] presented a general theory for free vibrations of sandwich beams with arbitrary boundary conditions. Complex natural frequencies (ω^{*}) were obtained in the form $\omega^{*2} = \omega^2 (1 + i\eta)$ where η is the loss factor. Interestingly, it was found that the modal loss factor bears a relationship with ω^2 which is independent of end conditions. Moreover, this relationship was found to be the same as that given by the previous work on infinite beam. However, the values of ω^2 depend on the boundary conditions

and as such the numerical values of η need to be determined separately for each boundary condition.

Mead and Markus [6] considered the forced vibration of a three layer damped sandwich beam with arbitrary boundary conditions. They used the concept of forced damped modes for the response calculation. Markus et al [7] also discussed numerical techniques for determination of modal loss factors and natural frequencies of such structures. The problem of damped sandwich plates with elastic constraints along one pair of edges was investigated by Mead [8] . He also investigated the free vibration of a damped sandwich plate on periodic supports [9].

All these works, mentioned above, consider beams of solid cross section for which the centroid and the shear centre coincide. For such structures the bending and torsional modes are decoupled.

As already mentioned, stringers are beam type structures with open cross sections for which the shear centre and the centroid usually do not coincide. In such cases there will be coupling between the bending and torsional modes of oscillation. Gere and Lin [10] presented an approximate method based on Rayleigh - Ritz formulation for determination of the coupled natural frequencies.

1.3 Objective and Scope of the Present Work

The major objective of the present work is to
provide a theoretical analysis for the free vibration charac-
teristics of thin walled open section beams with unconstrained
viscoelastic layer. As an example, the problem of a top hat
section with damping layer on the flanges is considered. The
base material is assumed to be nondissipative and the loss·
factor of the viscoelastic material is assumed to be indepen-
dent of frequency. Moreover the loss factor is assumed to be
the same in the extensional and shear modes of deformation.
The exact analysis of the free vibration characteristics of
thin walled open sections is presented in Chapter 2. Numeri-
cal results of natural frequencies are compared with those
obtained by the approximate method of Gere and Lin [10].

The analysis for the uncoupled bending vibration in
the plane of symmetry is essentially that of the transverse
vibration of beams with solid cross-section [2 to 9]. The
natural frequencies and modal loss factors are obtained in
close form in terms of geometric and material properties of
the beam.

The analysis for the coupled bending and torsional
oscillations require, as a first step, the determination of
the St. Venant's torsion constant and the warping rigidity
of the composite beam. These quantities turn out to be
complex quantities due to the presence of the dissipative

layer. The St. Venant torsion constant is determined by extending the membrane analogy of elastic sections to the composite section. The warping rigidity is derived in terms of the average warping function.

The coupled bending and torsional modes are governed by coupled eighth order differential equation. Assuming harmonic motion for the free vibration, the frequencies turn out to be complex. The real part is the natural frequency and the ratio of the imaginary part to the real part gives the modal loss factor.

The standard procedure of determining the frequency results in a frequency determinant with complex elements. The zeroes of this determinant determine the natural frequencies and modal loss factors. The complex arithmetic adds a dimension of difficulty to the determination of roots of the frequency equation. This difficulty is overcome by using a two dimensional Newton - Raphson technique. Numerical results are presented for various geometric and material parameters involved.

CHAPTER 2

FREE VIBRATION OF OPEN SECTION THIN WALLED BEAMS

2.1 Formulation of the Problem

Figure 2.1 shows a typical beam cross section considered in this thesis; where O is the shear centre and C is the centroid. X axis is the longitudinal axis through O forming a right handed coordinate system with Y and Z axes. In the following analysis v and w represent deflection along Y and Z axes respectively. ψ refers to the rotation of the cross section about X axis. The coordinate system $\chi\eta\zeta$ has its origin at C.

It can be readily seen that

$$w_c = w_o$$
$$v_c = v_o - c_z \psi \qquad (2.1)$$

where c_z is the distance of the centroid from the shear centre, the subscripts refer to the points under consideration.

The equation of motion can now be written as [10]

$$E I_\eta \frac{\partial^4 w_o}{\partial x^4} + \rho A \frac{\partial^2 w_o}{\partial t^2} = 0 \qquad (2.2)$$

$$E I_\zeta \frac{\partial^4 v_o}{\partial x^4} + \rho A \frac{\partial^2}{\partial t^2} (v_o - c_z \psi) = 0 \qquad (2.3)$$
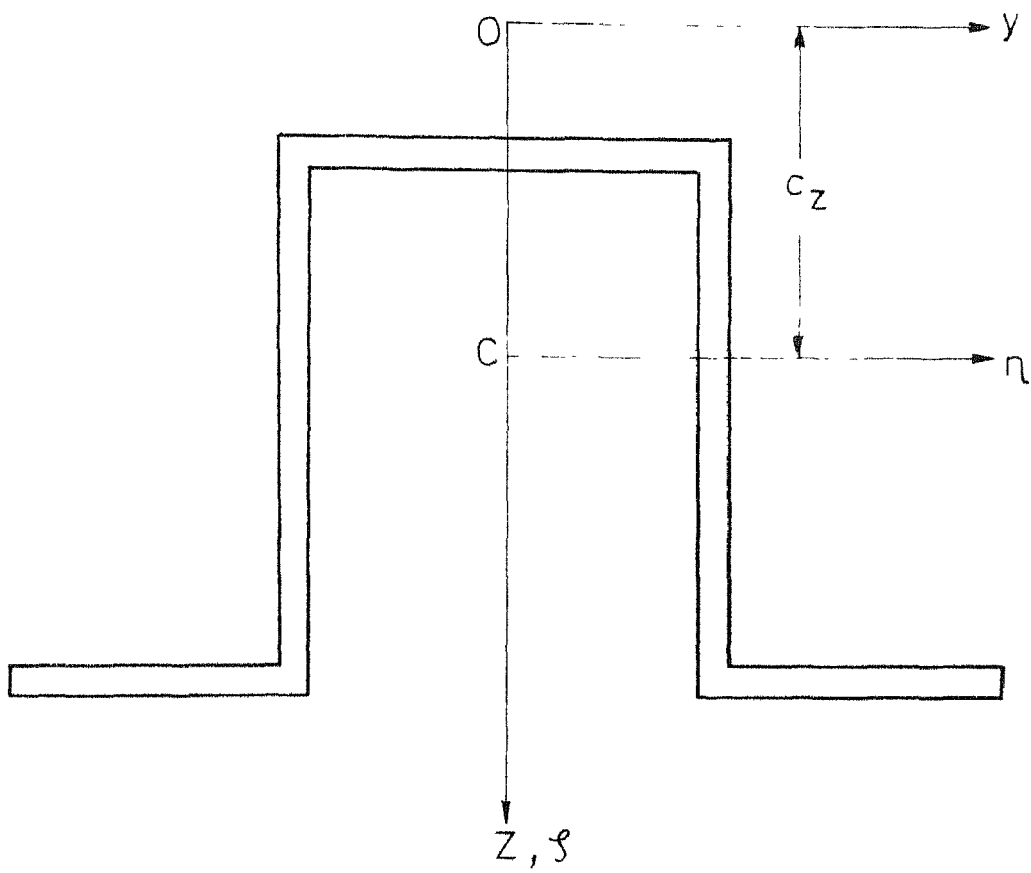
Fig.2·1 Typical beam cross section

$$E C_w \frac{\partial^4 \psi}{\partial x^4} - G C_s \frac{\partial^2 \psi}{\partial x^2} - \rho A \frac{\partial^2}{\partial t^2} (v_o - c_z \psi) c_z$$

$$+ \rho I_c \frac{\partial^2 \psi}{\partial t^2} = 0 \qquad (2.4)$$

where I_η and I_ζ are area moments of inertia of the cross section about η and ζ axes respectively. A, C_s and C_w are area of cross-section, Saint Venant's torsion constant and the warping constant. E and G are elastic and shear moduli of beam material. I_c is the polar moment of inertia of beam cross-section.

Equation (2.2) is the classical Euler's equation for vibration of the beam for which the results are well known.

Assuming harmonic motions for the free vibration

$$v_o = V_o (x) e^{i \omega t}$$

and $\psi = \psi_o (x) e^{i \omega t}$

equations (2.3) and (2.4) can be transformed, using equation (2.1) to

$$\frac{d^8 V_o}{dx^8} - \frac{G C_s}{E C_w} \frac{d^6 V_o}{dx^6} - \left(\frac{\rho A}{E I_\zeta} + \frac{\rho A c_z^2}{E C_w} + \frac{\rho I_c}{E C_w} \right) \omega^2 \frac{d^4 V_o}{dx^4}$$

$$+ \left(\frac{G C_s}{E C_w} \times \frac{\rho A}{E I_\zeta} \right) \omega^2 \frac{d^2 V_o}{dx^2} + \left(\frac{\rho I_c}{E C_w} \times \frac{\rho A}{E I_\zeta} \right) \omega^4 V_o = 0$$

$$(2.5)$$

In terms of nondimensional quantities, equation (2.5) can be rewritten as

$$\frac{d^8 V_o}{d\xi^8} + \alpha_1 \frac{d^6 V_o}{d\xi^6} + \Omega_n^2 \alpha_2 \frac{d^4 V_o}{d\xi^4} + \Omega_n^2 \alpha_3 \frac{d^2 V_o}{d\xi^2} + \Omega_n^4 \alpha_4 V_o = 0$$

(2.6)

The constants α_1, α_2 etc. are given in Appendix A, and Ω_n is the nondimensional natural frequency.

Assuming the solution $V_o(x) = \sum_{s=1}^{8} Q_s e^{\lambda_s x}$ for equation (2.6), the following characteristic equation is obtained for λ

$$\lambda^8 + \alpha_1 \lambda^6 + \alpha_2 \Omega_n^2 \lambda^4 + \alpha_3 \Omega_n^2 \lambda^2 + \alpha_4 \Omega_n^4 = 0 \qquad (2.7)$$

Applying appropriate boundary conditions at the two ends of the beam the frequency determinant (order 8 x 8) in the form

$$\text{Det } [A] = 0 \qquad (2.8)$$

is obtained.

The elements of the matrix A for simply supported and fixed end beams are given in Appendix A . The coupled natural frequencies, Ωn are obtained by using Newton - Raphson method.

2.2 Results and Discussion

Table 2.1 shows the first eight natural frequencies for the coupled vibration. The table also includes

the results obtained by the approximate method of Gere and Lin [10], which are found to be in close agreement. Table 2.2 presents the natural frequencies in the vertical (uncoupled) and in the coupled modes, nondimensionalised with respect to the same quantities. It is seen that some of the natural frequencies in the vertical mode are quite close to those in the coupled mode. This suggests the possibility of these modes being excited simultaneously. This behaviour has also been observed experimentally [11].

TABLE 2.1

COUPLED NATURAL FREQUENCIES BY EXACT AND APPROXIMATE

ANALYSIS

l_2 = 2.5400 cm

l_1 = 1.7780 cm

h = 2.9718 cm

t = 0.2032 cm

$$\Omega_n = \sqrt{\dfrac{\omega_n}{\dfrac{E\,I_\zeta}{\rho\,A\,l^4}}} \qquad \Omega_a = \sqrt{\dfrac{\omega_a}{\dfrac{E\,I_\zeta}{\rho\,A\,l^4}}}$$

where ω_n and ω_a are the natural frequencies by present analysis and approximate analysis respectively.

	END CONDITIONS		
	Simply Supported Ends		Fixed Ends
MODE	Natural Frequency by Present Analysis Ω_n	Natural Frequency by Approximate Analysis Ω_a [10]	Natural Frequency by Present Analysis Ω_n
1	5.40	5.40	10.13
2	17.92	20.86	26.81
3	20.85	23.91	46.23
4	38.51	47.59	84.50
5	67.21	74.56	126.98
6	81.60	84.92	174.91
7	104.23	109.67	232.42
8	149.40	154.12	248.54

TABLE   2.2

NATURAL FREQUENCIES IN COUPLED AND VERTICAL MODES
OF A SIMPLY SUPPORTED BEAM NONDIMENSIONALISED IN
THE SAME MANNER

l_2 = 2.5400 cm

l_1 = 1.7780 cm

h = 2.9718 cm

t = 0.2032 cm

$$\Omega_c = \frac{\omega_c}{\sqrt{\frac{E\,I_\eta}{\rho A\,l^4}}} \qquad \Omega_v = \frac{\omega_v}{\sqrt{\frac{E\,I_\eta}{\rho A\,l^4}}}$$

where Ω_c and Ω_v are natural frequencies in coupled and vertical modes respectively.

MODE	Frequency in Coupled Mode, Ω_c	Frequency in Vertical Mode, Ω_v
1	8.61	9.88
2	28.60	39.51
3	33.27	88.89
4	61.46	158.04
5	107.26	246.93
6	130.23	355.58
7	166.35	483.99
8	238.44	632.16

CHAPTER 3

EFFECT OF UNCONSTRAINED DAMPING LAYER ON
GEOMETRIC AND ELASTIC PROPERTIES

3.1 Shear Centre Location

When the damping layer is attached to the flanges of the cross-section as shown in Fig. 3.1 the shear centre of the composite cross-section will be shifted. The new position of the shear centre is determined by the following analysis.

Consider the bending of the section about the Z axis under the application of a shear load V in the Y direction through the shear centre O. AA and BB are two adjacent sections along the length of the beam, distance dx apart.

1 and 2 refer to the base material and the viscoelastic layer respectively. Consider a section CC at a distance y from the neutral axis Z. The unbalanced axial force due to the differential bending moment is equilibrated by the elemental shear force dF given by

$$dF = l_1 \int_{z_0}^{z_0 + t_1} (\sigma_{1B} - \sigma_{1A}) \, dz$$

$$+ l_1 \int_{z_0 + t_1}^{z_0 + t_1 + t_2} (\sigma_{2B} - \sigma_{2A}) \, dz \quad (3.1)$$

where σ refers to the bending stresses, with the subscripts indicating the material and section.

Fig. 3·1 Section of the composite beam

The bending moment at a section is resisted by both the base layer and the viscoelastic layer. Assuming the longitudinal strain at a section distant y from the neutral axis is the same for both, the portions of the bending moment resisted by each can be shown to be

$$M_1 = \frac{M E_1 I_{\zeta_1}}{E_1 I_{\zeta_1} + E_2^* I_{\zeta_2}} \qquad (3.2)$$

$$M_2 = \frac{M E_2^* I_{\zeta_2}}{E_1 I_{\zeta_1} + E_2^* I_{\zeta_2}} \qquad (3.3)$$

where M is the applied bending moment and I_{ζ_1}, I_{ζ_2}, the area moments of inertia about the neutral axis, and E_1 and E_2^* are the elastic modulus of the base material and the complex modulus of elasticity of the viscoelastic material.

From Eqns. (3.1) to (3.3) and using engineering bending theory it can be shown that the shear stresses in the two layers are

$$(\tau_{xy})_1 = \frac{V E_1 Q_1}{t_1 (E_1 I_{\zeta_1} + E_2^* I_{\zeta_2})}$$

$$(\tau_{xy})_2 = \frac{V E_2^* Q_2}{t_2 (E_1 I_{\zeta_1} + E_2^* I_{\zeta_2})} \qquad (3.4)$$

where Q_1 and Q_2 are the static moments about the neutral axis of the areas above the section at which the shear stresses are acting.

Considering the moment balance about a convenient point in the plane of the cross-section of all the shear forces the shear centre can be located. The final expression for the shear centre location is given in Appendix B . It should be noted that the shear centre position in this case is not only a function of the geometrical properties of the section but also depends on the material properties. Because of the complex modulus of the viscoelastic layer the location is given by a complex number.

3.2 Torsional Rigidity of the Two Layer Beam

In the case of thin walled open section beams, the applied torque is resisted by two different types of deformation. The first part corresponds to the torque balanced by shearing stresses due to pure torsion (St. Venant's torsion). The other part is the torque resisted by the warping stresses.

The St. Venant's torsional rigidity corresponding to the torque resisted due to pure torsion for the composite section is derived by an extension of the membrane analogy method.

Consider the equivalent membrane problem, namely that of the deflection of the membrane made of two materials of equivalent size (Fig. 3.2a) subjected to internal pressure. The membrane which is initially in the form of $\emptyset = 0$ will deform in the shape $\emptyset = \emptyset (z, y)$ as shown in Fig. 3.2 b.
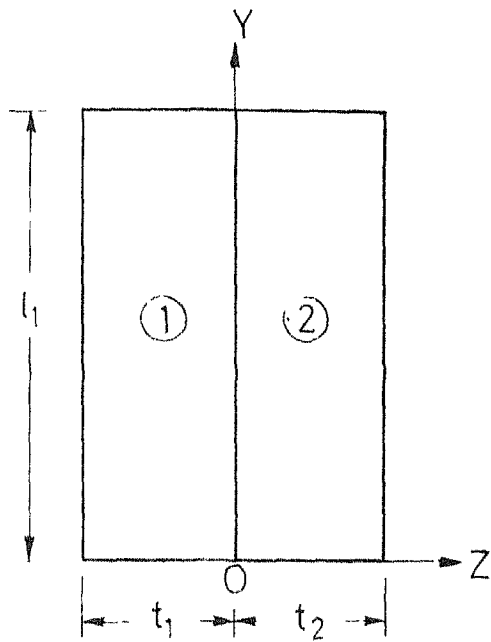
Fig. 3·2a Equivalent
membrane
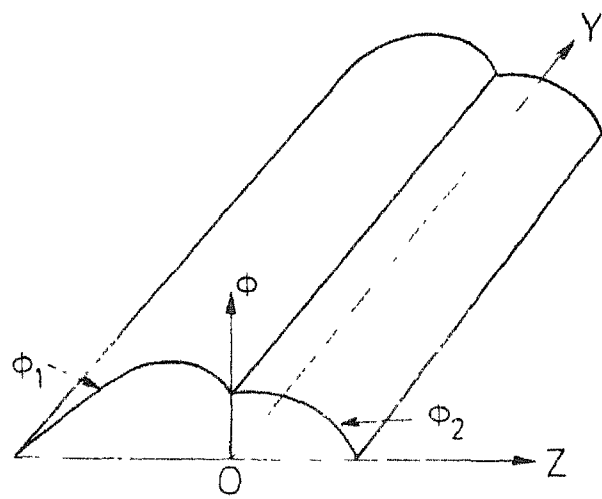
Fig. 3·2c Approximate shape of
deflected membrane
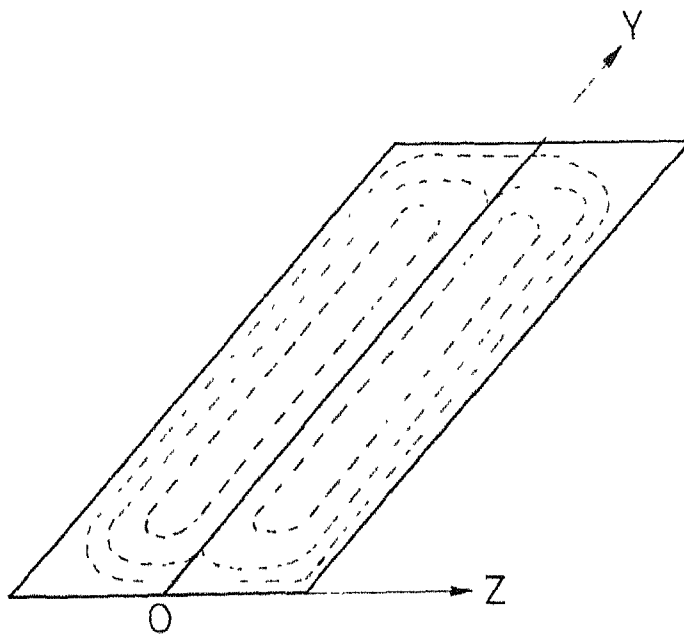
Fig. 3·2b Actual shape of deflected
membrane

If $l_1 \gg t_1$ and $l_1 \gg t_2$, the cross section of the membrane can be considered as independent of y except near the end as shown in Fig. 3.2c. ϕ_1 and ϕ_2 are the deflected surfaces of the membrane of material 1 and 2 respectively which also correspond to the Saint Venant's stress functions.

Let θ_o be the uniform twist along the length, then using the membrane analogy ϕ_1 and ϕ_2 are governed by the following equation,

$$\frac{\partial^2 \phi_1}{\partial z^2} = -2 G_1 \theta_o$$

$$\frac{\partial^2 \phi_2}{\partial z^2} = -2 G_2^* \theta_o \qquad (3.5)$$

where G_1 and G_2^* are respective shear moduli.

The shear stresses can be determined from the stress functions using the relations

$$(\tau_{xy})_1 = -\frac{\partial \phi_1}{\partial z} \quad \text{and} \quad (\tau_{xy})_2 = -\frac{\partial \phi_2}{\partial z} \qquad (3.6)$$

ϕ_1 and ϕ_2 can be found by integrating Eq. (3.5) and applying the following boundary conditions:

$$\phi_1(0) = \phi_2(0)$$
$$\phi_1(-t_1) = \phi_2(t_2) = 0$$

At $z = 0$, $(\gamma_{xy})_1 = (\gamma_{xy})_2$

i.e. $\left. \dfrac{1}{G_1} \dfrac{\partial \phi_1}{\partial z} \right|_{z=0} = \left. \dfrac{1}{G_2^*} \dfrac{\partial \phi_2}{\partial z} \right|_{z=0} \qquad (3.7)$

where γ_{xy} represents the shear strain.

The final forms of $\emptyset_1$ and $\emptyset_2$ turn out to be

$$\emptyset_1 = - G_1 \, \Theta_o \, (z^2 - t_1^2) + \mu G_1 \, \Theta_o \, (z + t_1)$$

$$\emptyset_2 = - G_2^* \, \Theta_o \, (z^2 - t_2^2) + \mu G_2^* \, \Theta_o \, (z - t_2) \tag{3.8}$$

$$\text{where} \quad \mu = \frac{G_2^* \, t_2^2 - G_1 \, t_1^2}{G_2^* \, t_2 + G_1 \, t_1}$$

The torque resisted by the shear stresses in the flanges induced by pure torsion is given by

$$T_f = 2 \int \int \emptyset \, dz \, dy$$

$$= 2 \int_{A_{1f}} \emptyset_1 \, d A_1 + 2 \int_{A_2} \emptyset_2 \, d A_2 \tag{3.9}$$

where A_{1f} and A_2 are the areas of cross-section of the flanges for material 1 and 2 respectively. The torsional rigidity of the entire composite beam including the torque resisted by the rest of the cross-section is given in Appendix B .

3.3 Warping Rigidity of the Two Layer Beam

The warping stress generated due to fibers non-uniform torsion, induce shearing stresses which results in a resistive torque.

The warping displacement w_d can be written as [17]

$$w_d = (\overline{w}_s - w_s) \, \frac{\partial \psi}{\partial x} \tag{3.10}$$

where $\quad \overline{w}_s$ = Average warping function,

$\qquad w_s$ = Warping function,

$\qquad \psi$ = Rotation of cross-section.

Since ψ varies along the length of the beam, adjacent cross sections will not be warped equally and there will be axial strain ε_x in the longitudinal fibres of the beam, given by

$$\varepsilon_x = \frac{\partial w_d}{\partial x} = (\overline{w}_s - w_s) \frac{\partial^2 \psi}{\partial x^2} \qquad (3.11)$$

Assuming no slipping at the interface, the axial strain should be the same in both elastic and visco-elastic parts. But the warping stresses produced due to the axial strain are different due to different elastic moduli of the two materials.

Assuming there is no lateral pressure between the longitudinal fibres, one can write

$$\sigma_{x_1} = E_1 (\overline{w}_s - w_s) \frac{\partial^2 \psi}{\partial x^2}$$

and
$$\sigma_{x_2} = E_2^* (\overline{w}_s - w_s) \frac{\partial^2 \psi}{\partial x^2} \qquad (3.12)$$

where σ_{x_1} and σ_{x_2} are the warping stresses in the two different layers of elastic moduli E_1 and E_2^*.

Figure 3.3a shows an element cut out from the flange of the elastic portion of the beam shown in Fig. 3.3b. Along the middle line, the stresses vary with distance s measured from the edge of the section and can be calculated
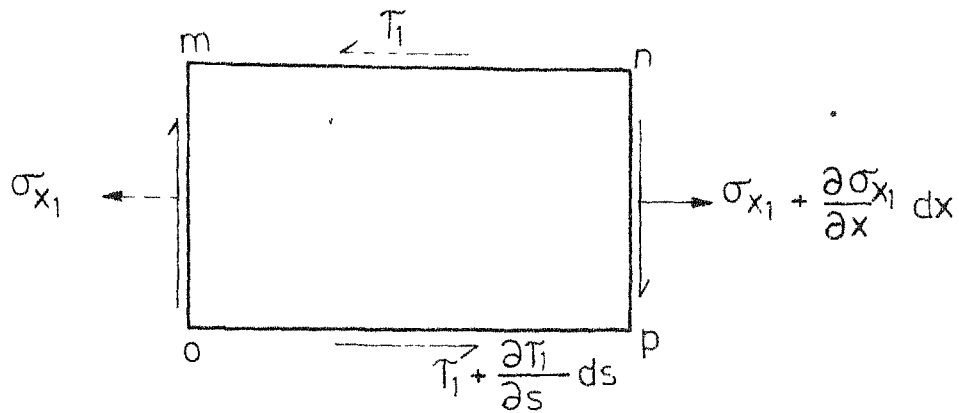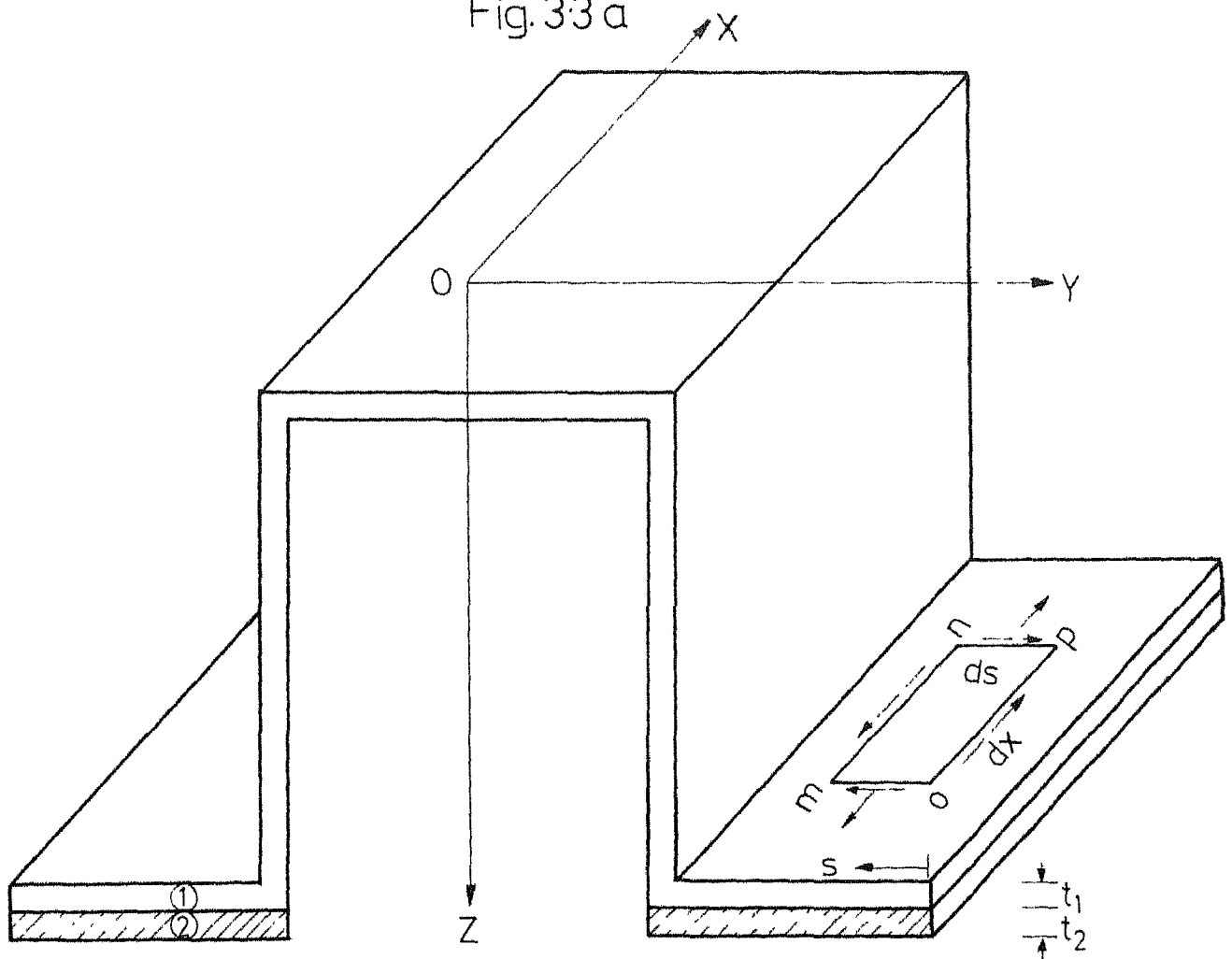
Fig. 3·3a

Fig. 3·3 b

Fig. 3·3   Stresses on an element on the flange
of the base material

from an equation of static equilibrium of the element

m n o p. Projecting all forces on to the x - axis, one can

write,

$$\frac{\partial (\tau_1 t_1)}{\partial s} \, ds \, dx + t_1 \, \frac{\partial \sigma_{x_1}}{\partial x} \, ds \, dx \, = \, 0 \qquad (3.13)$$

Integrating with respect to s and observing that

ψ is independent of s and that τ_1 vanishes for s = 0,

the expression for τ_1 can be written by using equation (3.12)

$$\tau_1 \, t_1 = - E_1 \, \frac{\partial^3 \psi}{\partial x^3} \, \int_0^s \, (\bar{w}_s - w_s) \, t_1 \, ds \qquad (3.14)$$

The resistive torque is obtained by summation along

the middle line of the section of the moments of the elemental

shear force about the shear centre. Therefore, the expression

for the warping rigidity M_1 for the elastic portion of the

beam can be written, using equation (3.14)

$$M_1 \, = \, - E_1 \, \frac{\partial^3 \psi}{\partial x^3} \, \int_0^m \{ \int_0^s \, (\bar{w}_s - w_s) \, t_1 \, ds \} r \, ds$$

$$(3.15)$$

where m is the perimeter of cross-section and r is

the perpendicular moment arm about the shear centre.

Integrating the last part of the integral of

equation (3.15) by parts and using $\int_0^m (\bar{w}_s - w_s) \, t_1 \, ds = 0,$

equation (3.15) can be written as

$$M_1 \, = \, - E_1 \, \frac{\partial^3 \psi}{\partial x^3} \, \int_0^m \, (\bar{w}_s - w_s)^2 \, t_1 \, ds$$

$$M_1 \, = \, - E_1 \, C_{w_1} \, \frac{\partial^3 \psi}{\partial x^3} \qquad (3.16)$$

where C_{W_1} is the warping constant for the elastic portion of the beam as given in Appendix B.

Similarly, one can proceed to find the expression for M_2, the warping rigidity for the visco-elastic part, as

$$M_2 = - E_2^* C_{W_2} \frac{\partial^3 \psi}{\partial x^3} \tag{3.17}$$

where C_{W_2} is the warping constant for visco-elastic portion of the beam and is given in Appendix B.

Table 3.1 presents some calculated values of the quantities discussed in the Chapter for a Typical Cross-Section.

TABLE 3.1

SHEAR CENTRE LOCATION, TORSIONAL RIGIDITY AND

WARPING RIGIDITY WITH VISCOELASTIC LAYER

$\dfrac{E_2}{E_1}$ = 0.001, $\beta = 1.0$ $l_1 = 3.0$ cm, $l_2 = 2.60$ cm,

h = 3.50 cm, $t_1 = 0.20$ cm,

E_1 = 70 x 10^4 Kgf/cm^2

$\dfrac{t_2}{t_1}$	Shear Centre Location (e)		Torsional Rigidity C_1		Warping Rigidity C_2	
	Real Part cm	Imag. Part cm	Real Part 10^{-5} Kgf $-cm^2$	Imag. Part 10^{-2} Kgf $- cm^2$	Real Part 10^{-7} Kgf $- cm^4$	Imag. Part 10^{-4} Kgf $-cm^4$
0.50	0.71677	−0.00076	0.10165	0.10443	0.70857	0.17797
1.0	0.71599	−0.00154	0.10193	0.38755	0.70876	0.36402
1.50	0.71520	−0.00233	0.10249	0.93828	0.70896	0.55827
2.0	0.71440	−0.00313	0.10340	1.8453	0.70916	0.76085

CHAPTER 4

FREE VIBRATION OF OPEN SECTION THIN WALLED BEAM

WITH UNCONSTRAINED DAMPING TREATMENT

AT THE FLANGES

4.1 Free Vibration in the Plane of Symmetry

4.1.1 Equation of Motion

Figure 4.1 shows the beam cross section with a visco-elastic layer on the flanges $n_1 - n_1$ is the neutral axis of the untreated beam section, $n_2 - n_2$ is that of the visco-elastic layer and $\eta - \eta$ is the composite neutral axis.

For displacement in Z direction the strain at $n_1 - n_1$ and $n_2 - n_2$ can be expressed as [5]

$$\varepsilon_1 = -D \frac{\partial^2 w}{\partial x^2}$$

(4.1)

$$\varepsilon_2 = H_{20} \frac{\partial^2 w}{\partial x^2}$$

where x is measured along the length of the beam and other quantities are explained in Figure 4.1.

The net extensional force on each layer can be obtained from the strains at their respective neutral axes as

$$F_1 = -E_1 A_1 D \frac{\partial^2 w}{\partial x^2}$$

and

(4.2)

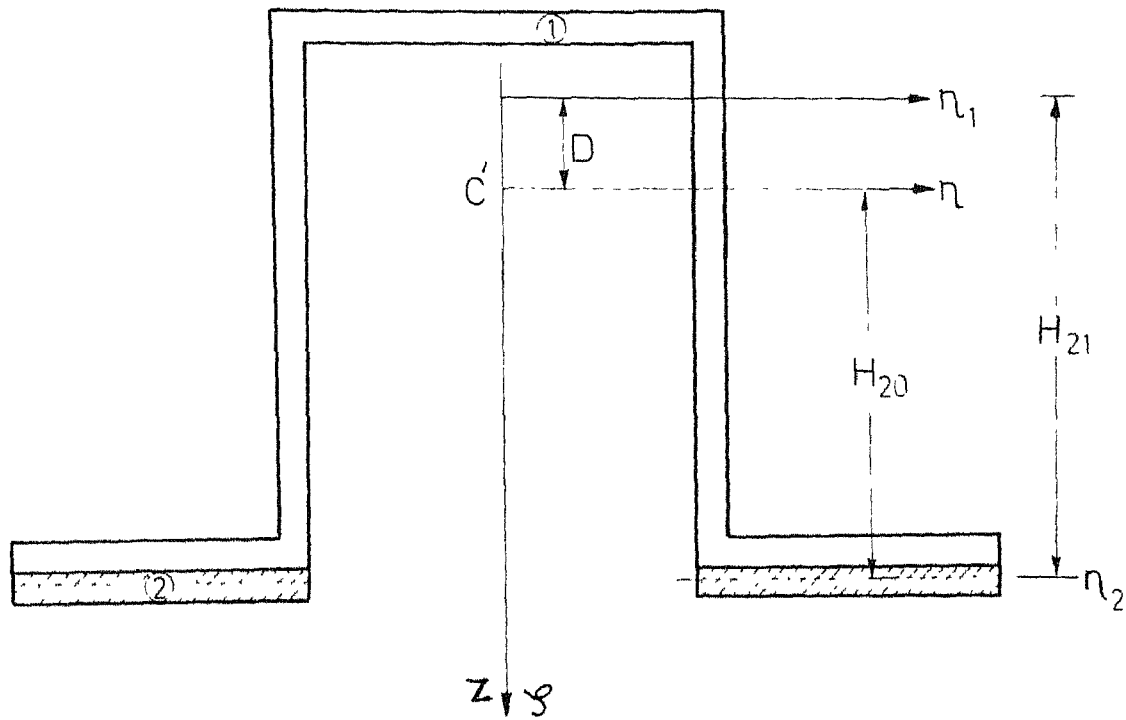$$F_2 = E_2^* A_2 H_{20} \frac{\partial^2 w}{\partial x^2}$$

Fig. 4.1 Top hat section with damping layer
on the flanges

As the total extensional force on the composite section is zero, one gets

$$F_1 + F_2 = (E_2^* A_2 H_{20} - E_1 A_1 D) \frac{\partial^2 w}{\partial x^2} = 0$$

or

$$E_2^* A_2 (H_{21} - D) = E_1 A_1 D$$

Thus the shift of the composite neutral axis from that of the original beam cross section, D, is given by

$$D = \frac{E_2^* A_2 H_{21}}{E_2^* A_2 + E_1 A_1} = D_R + i\, D_I \text{ (say)} \ldots \qquad (4.3)$$

with $E_2^* = E_2 (1 + i\beta)$, where β is the loss factor of the visco-elastic material, one gets

$$D_R = \frac{E_2 A_2 H_{21} (E_1 A_1 + E_2 A_2) + \beta^2 H_{21} E_2^2 A_2^2}{(E_1 A_1 + E_2 A_2)^2 + \beta^2 E_2^2 A_2^2} \qquad (4.4)$$

and

$$D_I = \frac{\beta H_{21} E_1 A_1 E_2 A_2}{(E_1 A_1 + E_2 A_2)^2 + \beta^2 E_2^2 A_2^2} \qquad (4.5)$$

The equation of motion can be derived by using the relation

$$\frac{\partial^2 M}{\partial x^2} = - (\rho_1 A_1 + \rho_2 A_2) \frac{\partial^2 w}{\partial t^2} \qquad (4.6)$$

The expression for the bending moment M can be written as

$$M = M_{11} + F_1 (-D) + M_{22} + F_2 H_{20}$$

where $M_{11} = E_1 I_{\eta_{11}} \dfrac{\partial^2 w}{\partial x^2}$

$$(4.7)$$

and $M_{22} = E_2^* I_{\eta_{22}} \dfrac{\partial^2 w}{\partial x^2}$

with $I_{\eta_{11}}$ and $I_{\eta_{22}}$ as the second moments area of the layers about their own neutral planes. Using equations (4.2), (4.6) and (4.7) the final equation of motions is obtained as

$$B (1 + i \nu) \frac{\partial^4 w}{\partial x^4} = - \rho A \cdot \frac{\partial^2 w}{\partial t^2} \qquad (4.8)$$

where $\rho A = \rho_1 A_1 + \rho_2 A_2$

$$B = E_1 \{ I_{\eta_{11}} + A_1 (D_R^2 - D_I^2) \} + E_2 \{ I_{\eta_{22}} +$$

$$A_2 (H_{21}^2 + D_R^2 - D_I^2 - 2 D_R H_{21} - 2 \beta D_I (D_R - H_{21}) \}$$

$$(4.9)$$

and

$$\nu B = 2 A_1 E_1 D_R D_I + 2 A_2 E_2 D_I (D_R - H_{21}) +$$

$$\beta E_2 \{ I_{\eta_{22}} + A_2 (H_{21}^2 + D_R^2 - D_I^2 - 2 D_R H_{21}) \}$$

$$(4.10)$$

Now, equation (4.8) is simply that of a hysteritically damped beam. So natural frequencies and loss factors at different modes for various boundary conditions can simply be written as follows:

For simply supported ends

$$\omega_n^2 = \frac{n^4 \pi^4}{1^4} \frac{B}{\rho A} \; , \quad n = 1, 2, 3, \ldots$$

(4.11)

and $\eta = \nu$

For clamped clamped ends

$$\omega_n^2 = \frac{(n + \frac{1}{2})^4 \pi^4}{1^4} \frac{B}{\rho A}$$

(4.12)

and $\eta = \nu$

If $E_2 \ll E_1$, as is usually the case, B and ν can be approximated from Eqs. (4.9) and (4.10) as

$$B \simeq E_1 I_{\eta_{11}} + E_2 (I_{\eta_{22}} + A_2 H_{21}^2)$$

(4.13)

and $\eta = \nu \simeq \beta \dfrac{E_2}{E_1} \dfrac{I_{\eta_{22}} + A_2 H_{21}^2}{I_{\eta_{11}} + E_2/E_1 \{ (I_{\eta_{22}} + A_2 H_{21}^2) \}}$

(4.14)

4.1.2 Numerical Results and Discussion

It can easily be seen from Eq. (4.11) and (4.12) that the loss factor in this mode of vibration in the plane of symmetry, is independent of both the end conditions and the mode number.

Figures 4.2 and 4.3 show typical values of the loss factor for various values of t_2/t_1, E_2/E_1 and the loss factor of visco-elastic material β . The following dimensions are used for the cross section of the elastic
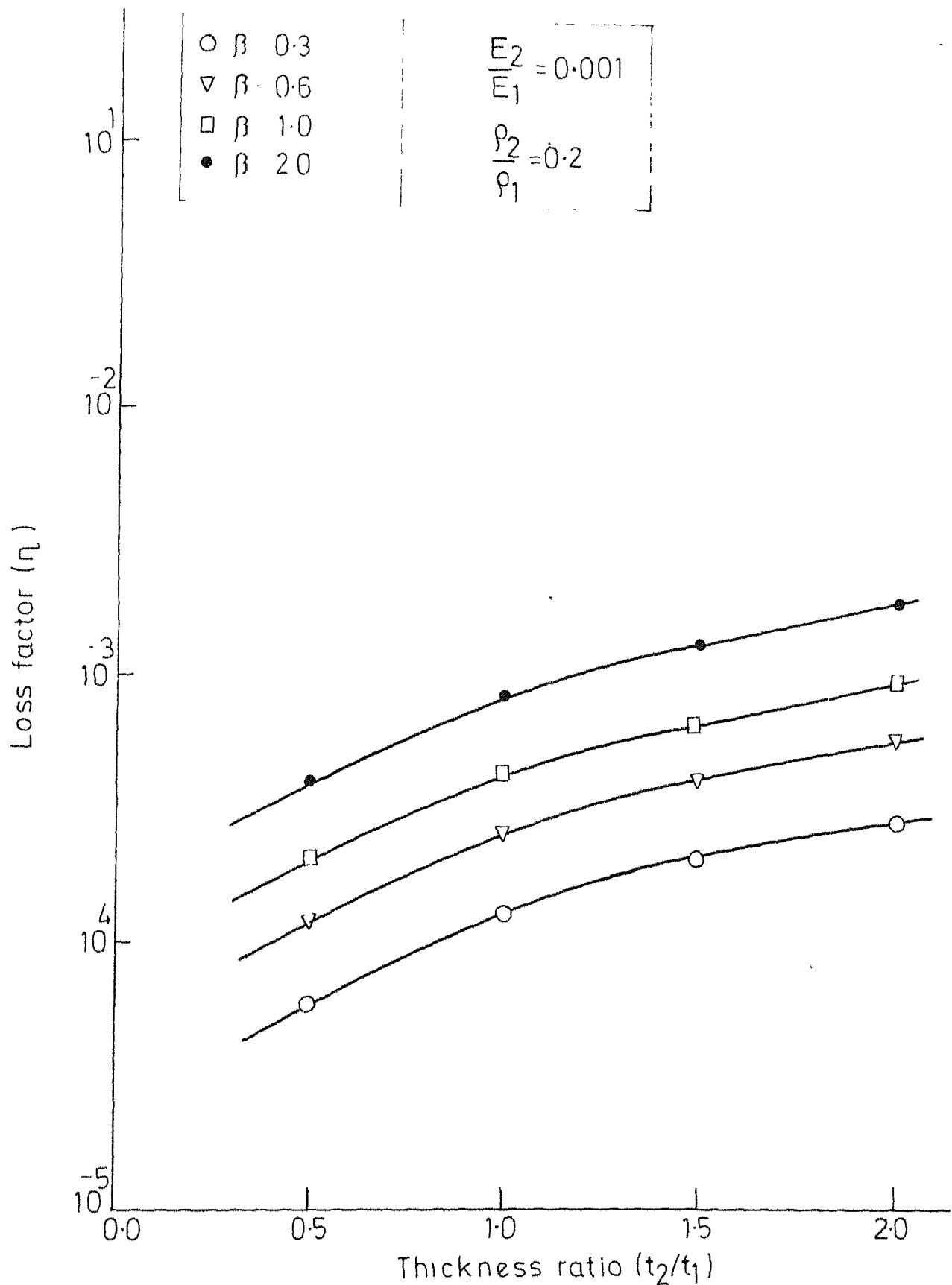
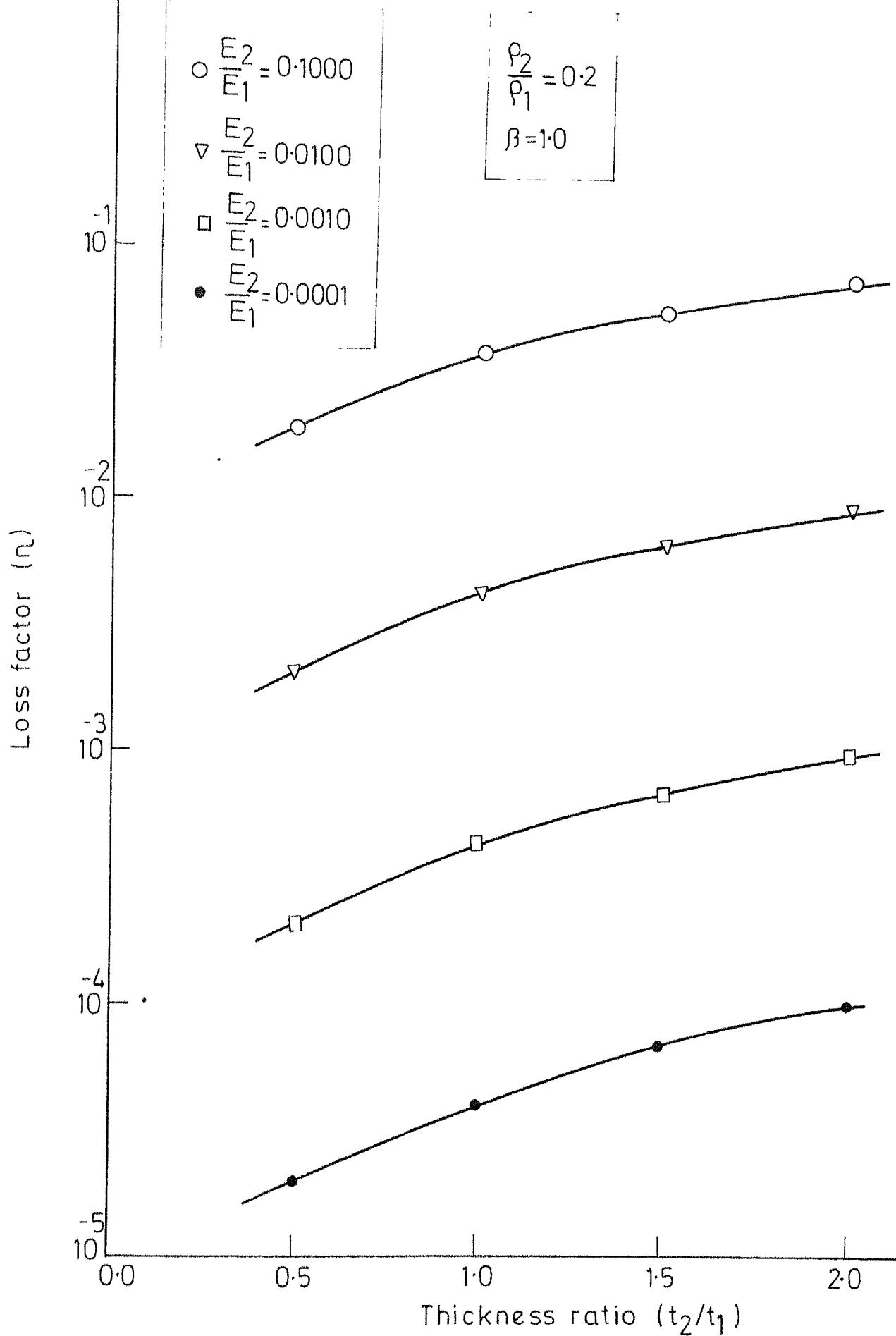Fig.4·2 Variation of loss factor with thickness ratio in vertical mode of vibration

Fig.43 Variation of loss factor with thickness ratio in vertical mode of vibration

layer, $l_1 = 2.00$ cm, $l_2 = 2.60$ cm, $h = 3.5$ cm and $t_1 = 0.20$ cm. As expected from the approximate expression (4.14), the composite loss factor η is seen to be almost proportional to E_2/E_1 and also proportional to β. The nature of variation of η with t_2/t_1 is also as predicted by Eq. (4.14).

4.2 Free Vibration in Coupled Bending Torsion Mode

4.2.1 Equation of Motion

Consider the top hat section with the damping layer in its flanges as shown in Figure 4.4. 0 and C respectively are the shear centre and the mass centre of composite section. Let v_c and v_o denote the displacements of C and 0 along the Y axis respectively. It is obvious that

$$v_c = v_o - c_z \psi \qquad \cdots \qquad (4.15)$$

where c_z is the distance of the mass centre from the shear centre. Considering the equilibrium of elastic and inertia forces in Y direction in one hand and the moment equilibrium about a longitudinal axis through the shear centre on the other, the following equations of motion are obtained.

$$(E_1 I_{\zeta_1} + E_2^* I_{\zeta_2}) \frac{\partial^4 v_o}{\partial x^4} + (\rho_1 A_1 + \rho_2 A_2) \frac{\partial^2 v_c}{\partial t^2} = 0$$
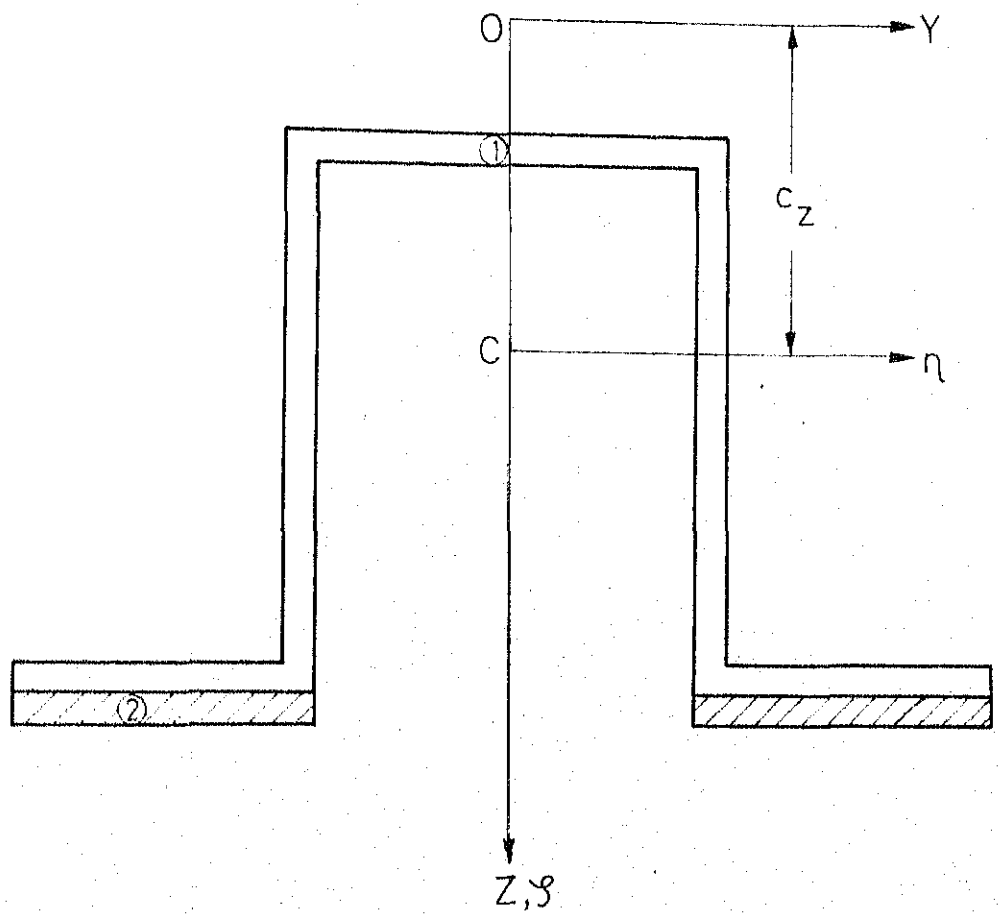
$$(4.16)$$

Fig.4·4 Cross section of composite beam

$$C_2 \frac{\partial^4 \psi}{\partial x^4} - C_1 \frac{\partial^2 \psi}{\partial x^2} - (\rho_1 A_1 + \rho_2 A_2) \frac{\partial^2 v_c}{\partial t^2} c_z$$

$$+ (\rho_1 I_{c_1} + \rho_2 I_{c_2}) \frac{\partial^2 \psi}{\partial t^2} = 0 \qquad (4.17)$$

where E_1 and E_2^* are Young's modulus of elasticity, I_{ζ_1} and I_{ζ_2} are area moments of inertia about ζ axis, A_1 and A_2 are areas of cross-section, ρ_1 and ρ_2 are mass densities, I_{c_1} and I_{c_2} are polar moments of inertia about a longitudinal axis. Subscripts 1, and 2 refer to the base material and viscoelastic layer. C_1, C_2 are the complex torsional rigidity and warping rigidity respectively of the composite cross section as derived in Chapter 3.

Assuming harmonic solution of the form

$$v_o = V_o (x) e^{i\omega t}$$

$$\psi = \psi_o (x) e^{i\omega t}$$

and using the relation (4.15) for eliminating ψ, the equation of motion can be transformed into the eight order ordinary differential equation in nondimensional form as

$$\frac{d^8 V_o}{d \xi^8} + \alpha_1 \frac{d^6 V_o}{d \xi^6} + \Omega_c^2 \alpha_2 \frac{d^4 V_o}{d \xi^4} + \Omega_c^2 \alpha_3 \frac{d^2 V_o}{d \xi^2}$$

$$+ \Omega_c^4 \alpha_4 V_o = 0 \qquad (4.18)$$

where α_1, α_2, α_3, α_4 and Ω_c^2 are given in Appendix C. The final form of equation (4.18) is exactly similar to

the equation (2.6) for the beam without the layer. But α_1, α_2, α_3, α_4 and Ω_c^2 are complex quantities in this case due to the presence of viscoelastic layer. In order to avoid confusion, let these complex natural frequencies be denoted as $\Omega_c^{*2} = \Omega_c^2 (1 + i\eta)$ where the real part Ω_c^2 is referred to as the natural frequency and η is the modal loss factor.

4.2.2 Frequency and Loss Factor Determination

Assuming a solution of the form

$$V_o(x) = \sum_{s=1}^{8} Q_s e^{\lambda_s x}$$

and substituting into the differential equation the following characteristic polynomial equation for λ is obtained

$$\lambda^8 + \alpha_1 \lambda^6 + \alpha_2 \Omega_c^{*2} \lambda^4 + \alpha_3 \Omega_c^{*2} \lambda^2 + \alpha_4 \Omega_c^{*4} = 0$$

(4.19)

Applying appropriate boundary conditions at the two ends of the beam the frequency equation is obtained in the form of

$$\text{Det } [A] = 0 \tag{4.20}$$

where the elements of **matrix** A are given in Appendix C.

The solution of the determinental equation in this case is much **more** complicated as compared to that without the viscoelastic layer. This is so because of

the cumbersome complex arithmetic involved and the inherent
numerical problems associated with it. This difficulty is
overcome by splitting the determinant into its real and
imaginary parts and setting these separately equal to zero.
The real and imaginary parts of the determinant are consi-
dered as function of two variables Ω_R^2, $\eta\,\Omega_R^2$ namely the
real and imaginary parts of the complex natural frequency
squared. The zeros of the functions are obtained by employ-
ing a two dimensional Newton - Raphson procedure. The itera-
tions in the Newton - Raphson procedure proceeds according
to the following sequence.

Let

$$A_R\ (x,\ y)\ =\ 0 \tag{4.21}$$

$$A_I\ (x,\ y)\ =\ 0 \tag{4.22}$$

where $x = \Omega_R^2$ and $y = \Omega_R^2\,\eta$

A_R and A_I are the real and imaginary parts of
determinental equation. Then, the iterations for the roots
of Equations (4.21) and (4.22) are

$$(x)_{j+1}\ =\ (x)_j\ +\ \left(\frac{A_I\,A_{R_y}\ -\ A_R\,A_{I_y}}{A_{R_x}\,A_{I_y}\ -\ A_{R_y}\,A_{I_x}}\right)_j$$

and

$$(y)_{j+1}\ =\ (y)_j\ +\ \left(\frac{A_R\,A_{I_x}\ -\ A_I\,A_{R_x}}{A_{R_x}\,A_{I_y}\ -\ A_{R_y}\,A_{I_x}}\right)_j$$

where suffixes x and y indicate partial differentiation
with respect to x and y respectively (for example

$\Lambda_{R_x} = \dfrac{\partial \Lambda_R}{\partial x}$, $\Lambda_{R_y} = \dfrac{\partial \Lambda_R}{\partial y}$ and so on). The subscript j

indicates that the concerned functions are evaluated at the point $(x, y)_j$. The required partial derivatives in the iterations are computed by a central difference scheme. Starting from the lower end of frequency scale the iterations are continued to obtain the natural frequencies of various orders successively. The convergence criterion for each natural frequency and loss factor are specified in terms of the percentage change in the values in consecutive iteration and the absolute value of the determinant.

The above scheme converged in most of the cases within six or seven iterations. The initial starting point for the variables did not present any problem in almost all the cases. However the determinant values vary over a wide range, with frequency. This presented some numerical problems of dealing with very large numbers. This problem is alleviated by suitably scaling the determinant value at the begining of the iteration scheme for the determination of a particular modal frequency.

4.2.3 Numerical Results and Discussion

Numerical results are obtained, using the analysis presented in 4.2.2, for the following dimensions and properties of the elastic layer:

l_1 = 2.00 cm, l_2 = 2.60 cm, t_1 = 0.20 cm and

h = 3.50 cm, ρ_1 = 2.7×10^{-6} Kgf - sec ^{2}/cm^4,

E_1 = 70 x 10^4 Kgf /cm^2, G_1 = 28 x 10^4 Kgf/cm^2,

l = 62.00 cm.

Table 4.1 presents the first eight natural frequencies and modal loss factors for a set of typical values of the parameters involved. It is seen, unlike in the case of vibration in the plane of symmetry, that the loss factor depends on the end conditions as well as modal number. This is due to the shearing of the viscoelastic layer caused by the coupling of bending and twisting modes. This fact has also been observed in the case of beams with solid cross-sections having constrained damping layer.

For both types of end conditions the loss factor in the first mode is seen to be considerably higher than those at higher modes. No definite trend in the variation of loss factor is observed with the modal numbers. At this stage, no attempt has been made to have physical justification for this behaviour. The mode shapes are very complicated to visualize any pattern of deformation for the damping layer. Hence it is suggested to calculate individually the loss factor in the required mode.

Figures 4.5 and 4.6 show the variation of loss factor with thickness ratio $(\frac{t_2}{t_1})$ for typical ratios of $\frac{E_2}{E_1}$ and $\frac{\rho_2}{\rho_1}$ and β for simply supported and clamped ends. It is seen that in the case of coupled modes also the nature of variation with $\frac{t_2}{t_1}$ is very similar to that observed in the vertical mode (shown in Fig. 4.2). The modal loss factor also appears to vary linearly with β , the loss factor of the viscoelastic material. As already observed in Table 4.1, the loss factor in the first mode always

TABLE 4.1

NATURAL FREQUENCIES AND MODAL LOSS FACTORS IN

COUPLED VIBRATION

$$\frac{t_2}{t_1} = 1.50, \qquad \frac{\rho_2}{\rho_1} = 0.20 \qquad l_1 = 2.00 \text{ cm}, \qquad l_2 = 2.60 \text{ cm}$$

$$\frac{E_2}{E_1} = 0.001, \qquad \beta = 1.00 \qquad t_1 = 0.20 \text{ cm}, \qquad h = 3.50 \text{ cm}$$

The nondimensional coupled natural frequency

$$\Omega_c^2 = \frac{\omega^2}{\dfrac{E_1 I_{\zeta_1} + E_2 I_{\zeta_2}}{(\rho_1 A_1 + \rho_2 A_2) l^4}} \qquad \text{where } \omega \text{ is the natural frequency}$$

$\eta =$ the composite loss factor.

MODE NO	SIMPLY SUPPORTED ENDS		FIXED ENDS	
	Ω_c	η	Ω_c	η
1	3.85778	0.00350	7.56462	0.00172
2	13.37329	0.00175	20.23136	0.00129
3	16.86532	0.00124	39.20238	0.00108
4	29.11707	0.00126	65.61231	0.00103
5	51.14014	0.00106	103.62929	0.00098
6	66.50152	0.00101	133.62726	0.00090
7	79.45019	0.00097	177.67156	0.00088
8	114.04927	0.00092	202.95039	0.00096

turns out to be higher than that in the second mode. Comparing the values of loss factors from Figs. 4.5 and 4.2, (for the same values of the parameters involved), it can be said that the unconstrained layer is more effecting in damping the lower order coupled modes.

From Figs. 4.7 and 4.8 it is seen again that the modal loss factor varies linearly with $\frac{E_2}{E_1}$. This trend was also observed for the vibration in the plane of symmetry (shown in Fig. 4.3).

Figures 4.9 and 4.10 show that the loss factor is virtually independent of $\frac{\rho_2}{\rho_1}$ in its feasible range. The obvious suggestion is that one should go for light viscoelastic materials so that the increase in weight is minimum with the damping layer.

Figures 4.11 to 4.16 show the changes in the natural frequencies with various parameters.

It can be noted that the natural frequency is virtually independent of β . For reasonable values of $\frac{E_2}{E_1}$ ($\simeq$ .001), the frequency is lowered with higher thickness ratio as the mass is increased without almost any change in bending rigidity. However, with $\frac{E_2}{E_1} \simeq$ .1, The increase in mass can be offset by the increase in rigidity so that the natural frequency increases with increasing thickness ratio. Figures 4.15 and 4.16 suggest the obvious results of lowering natural frequencies with increasing thickness ratio, the effect being more pronounced with higher values of $\frac{\rho_2}{\rho_1}$.
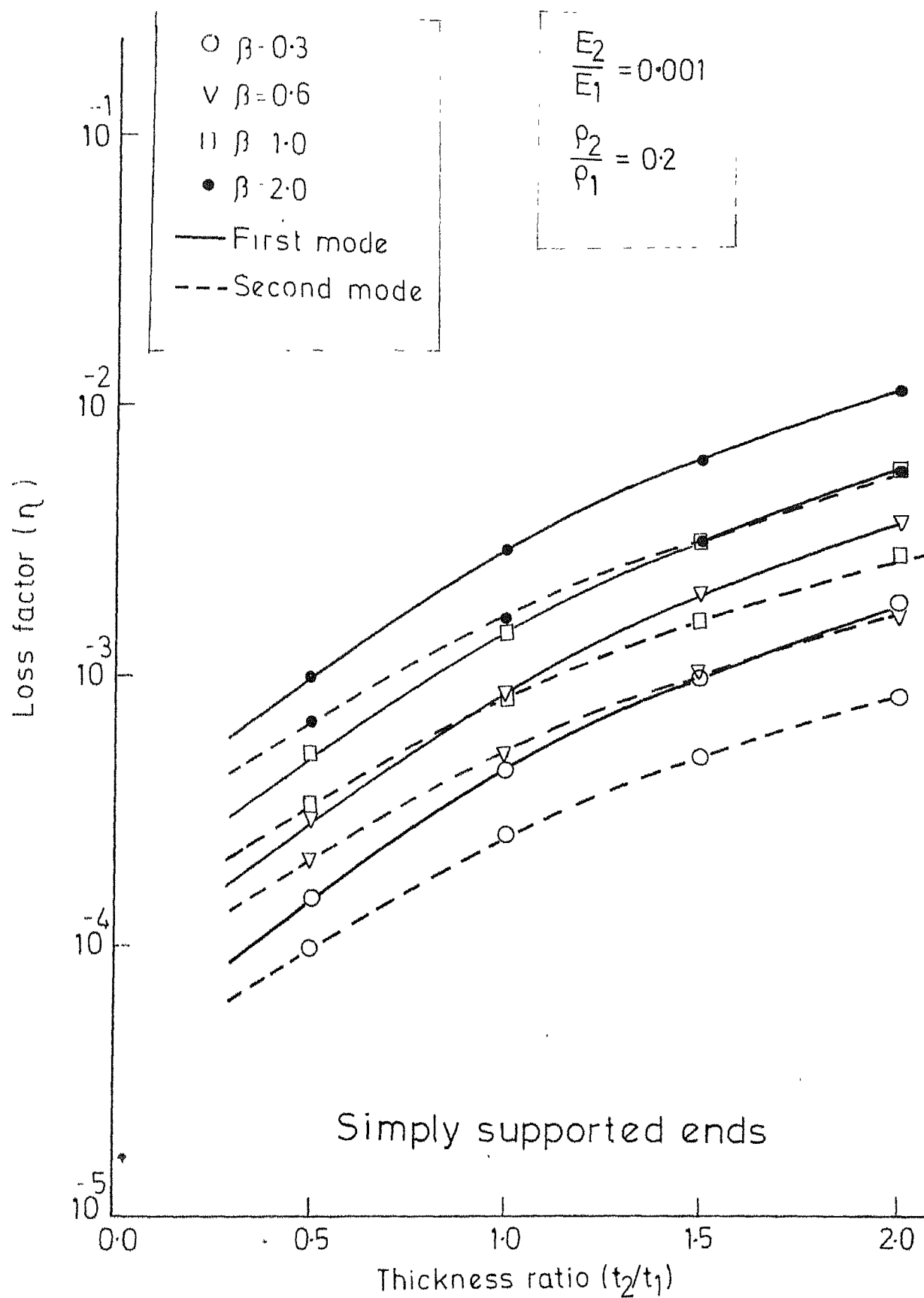
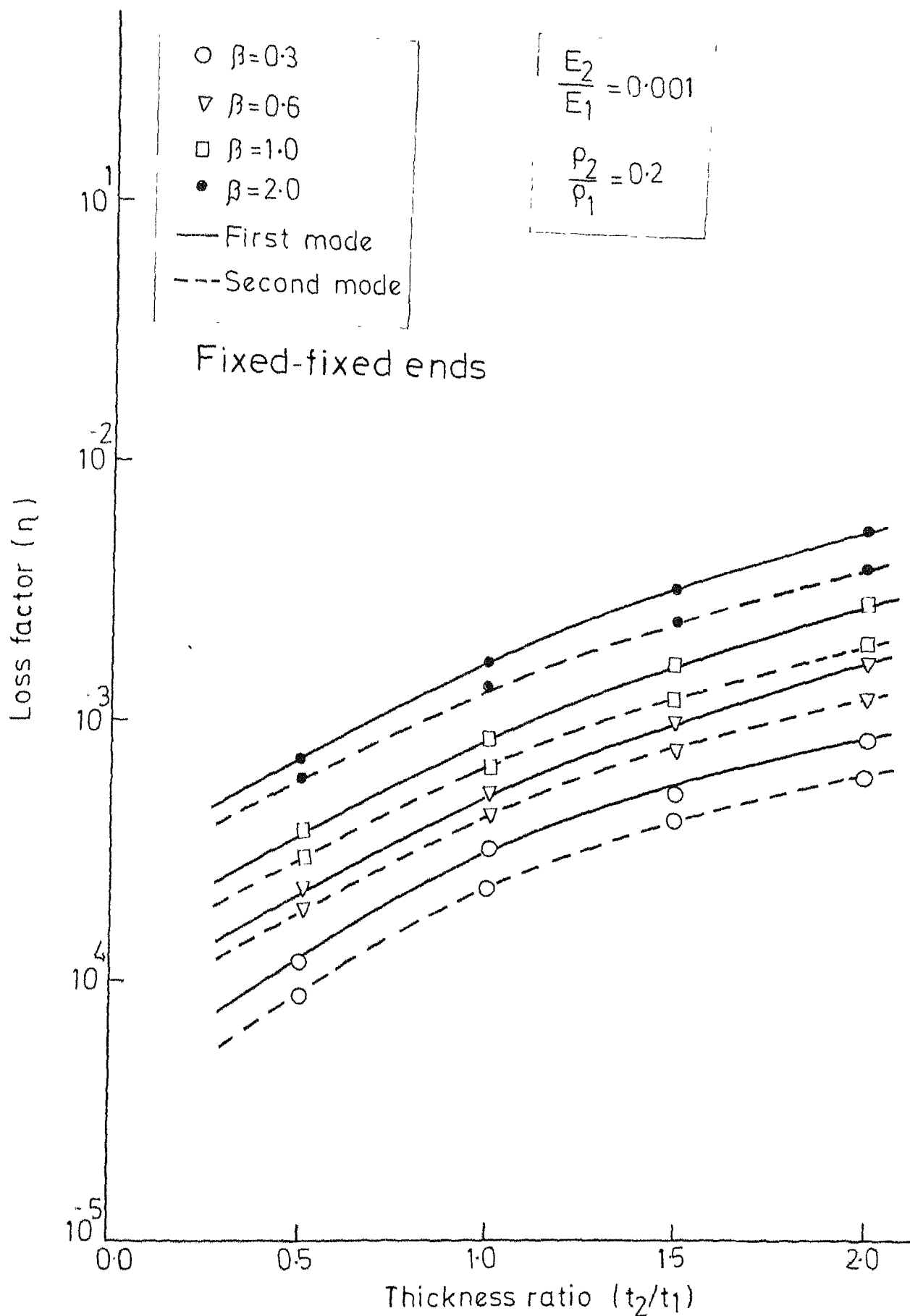Fig.4·5 Variation of loss factor with thickness ratio

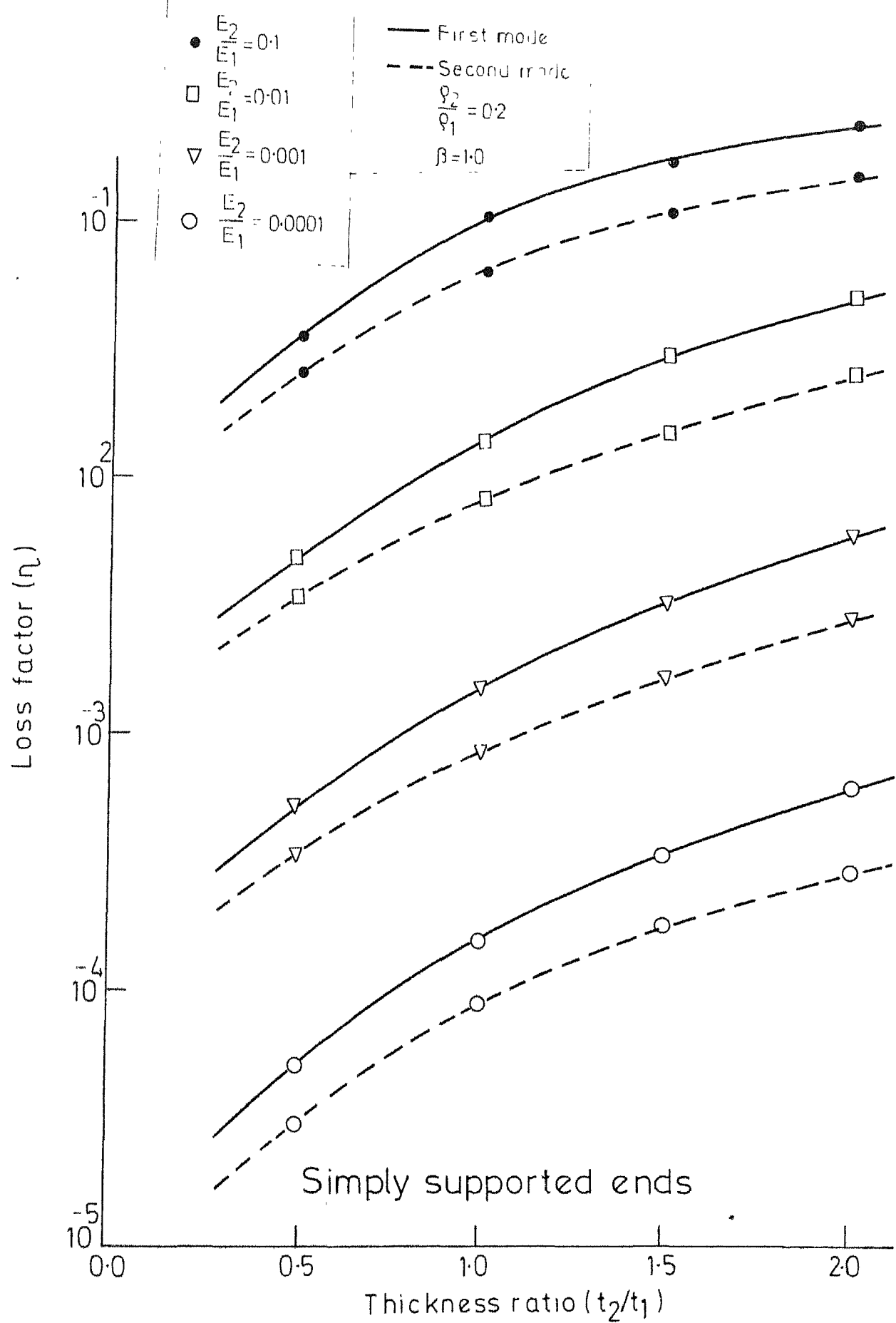Fig. 4·6 Variation of loss factor with thickness ratio

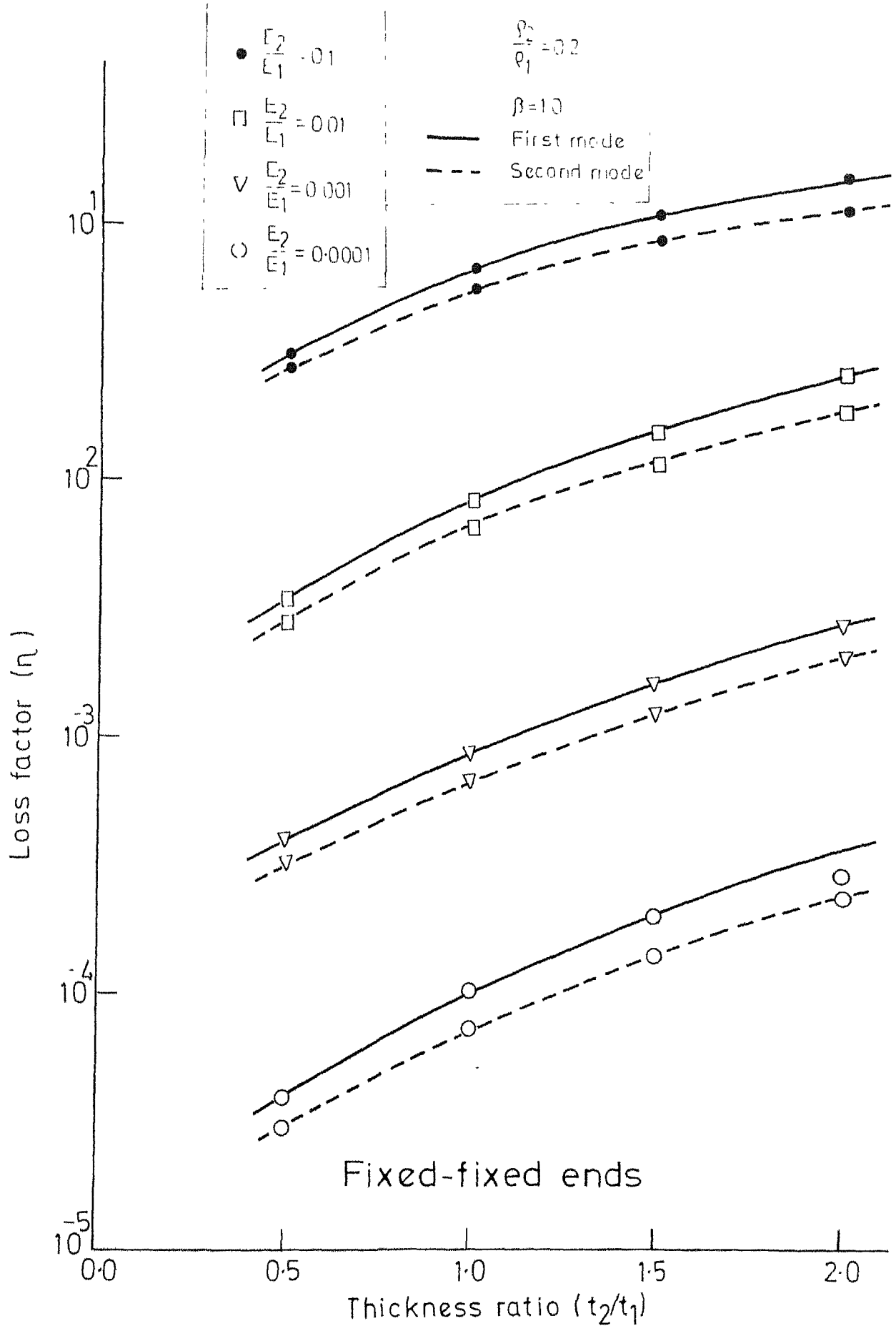Fig. 4·7 Variation of loss factor with thickness ratio

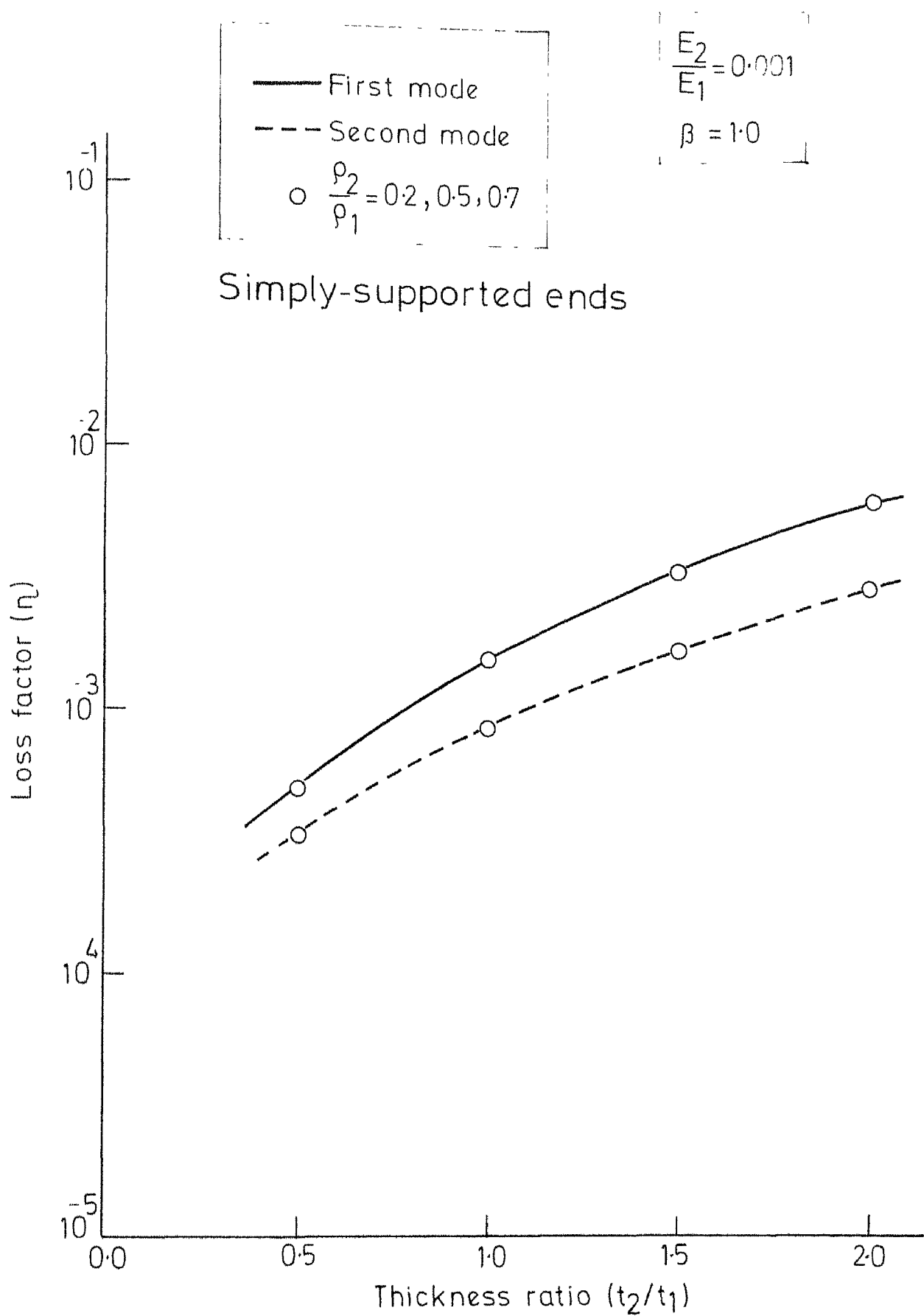Fig. 4·8 Variation of loss factor with thickness ratio

Fig. 4·9 Variation of loss factor with thickness ratio
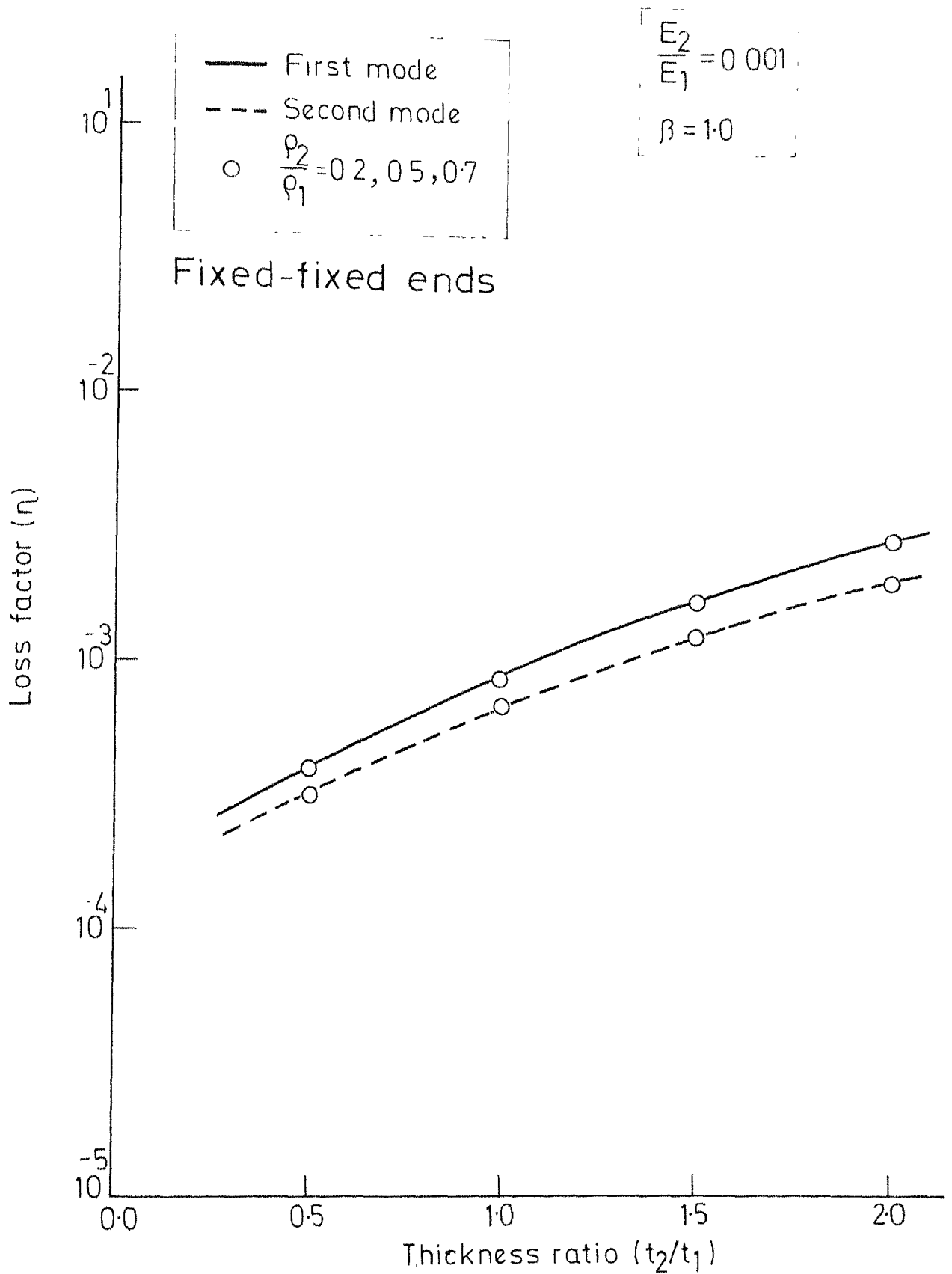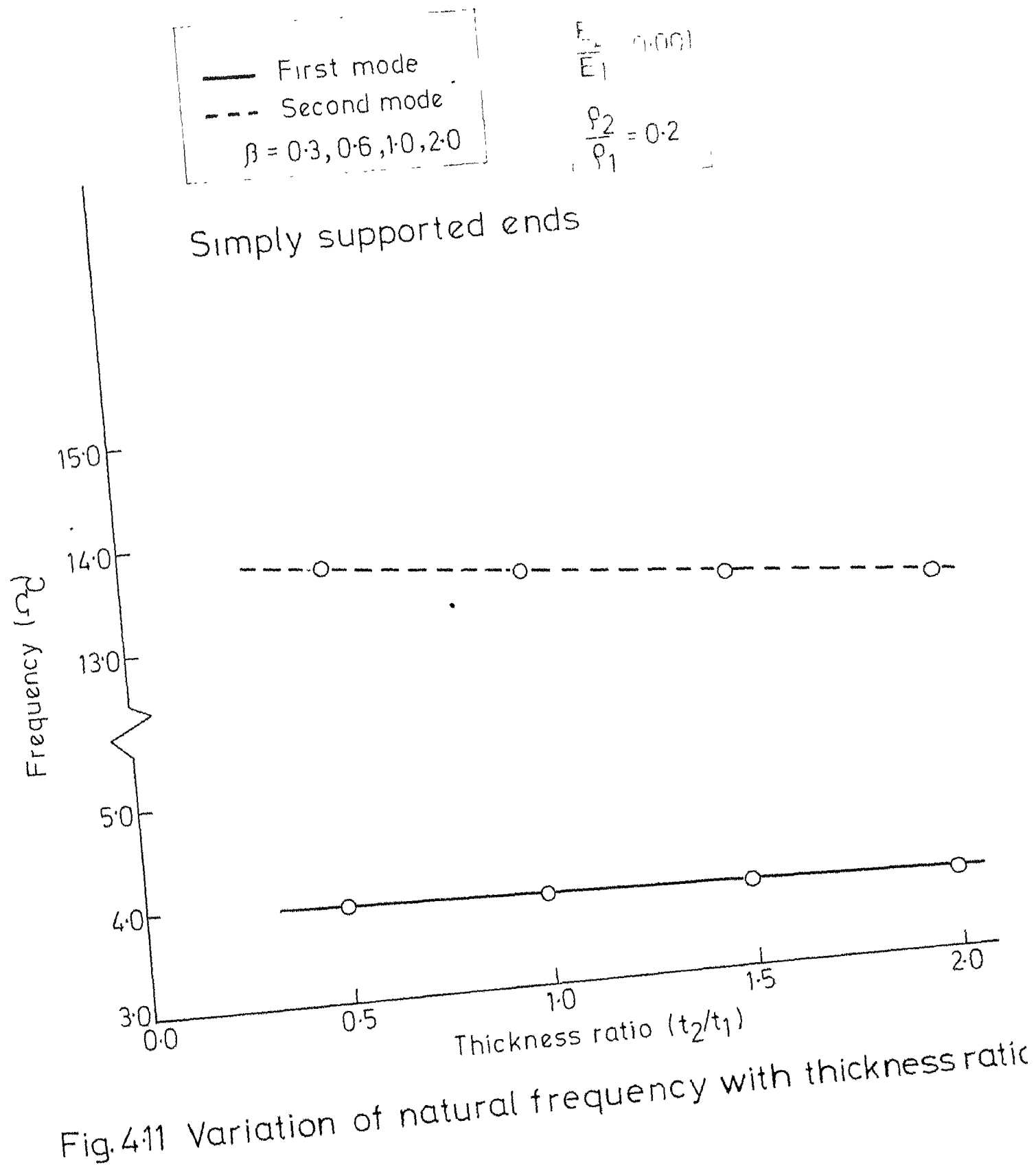
Fig. 4·10 Variation of loss factor with thickness ratio

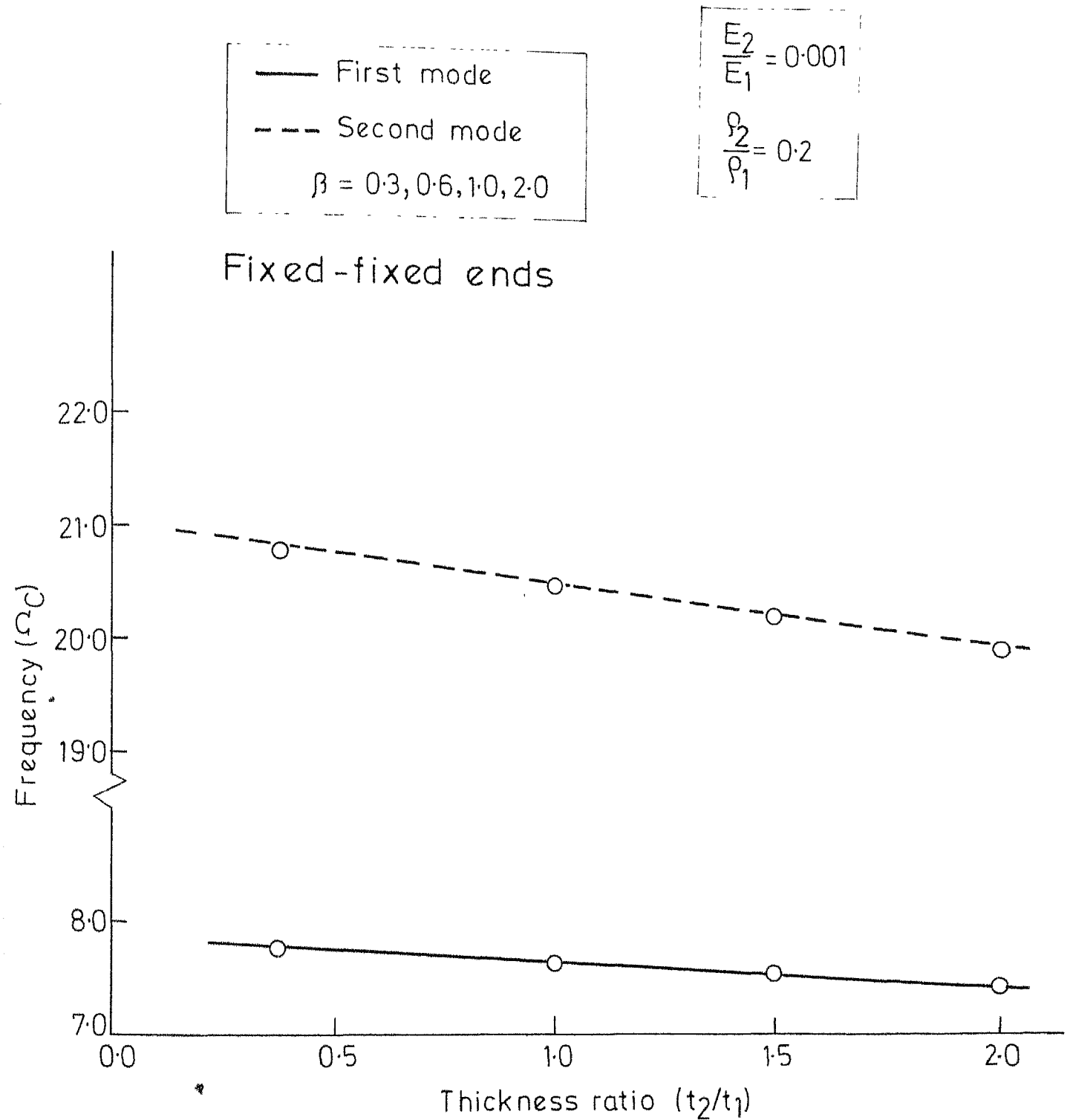Fig. 4.11 Variation of natural frequency with thickness ratio

Fig. 4.12 Variation of natural frequency with thickness ratio
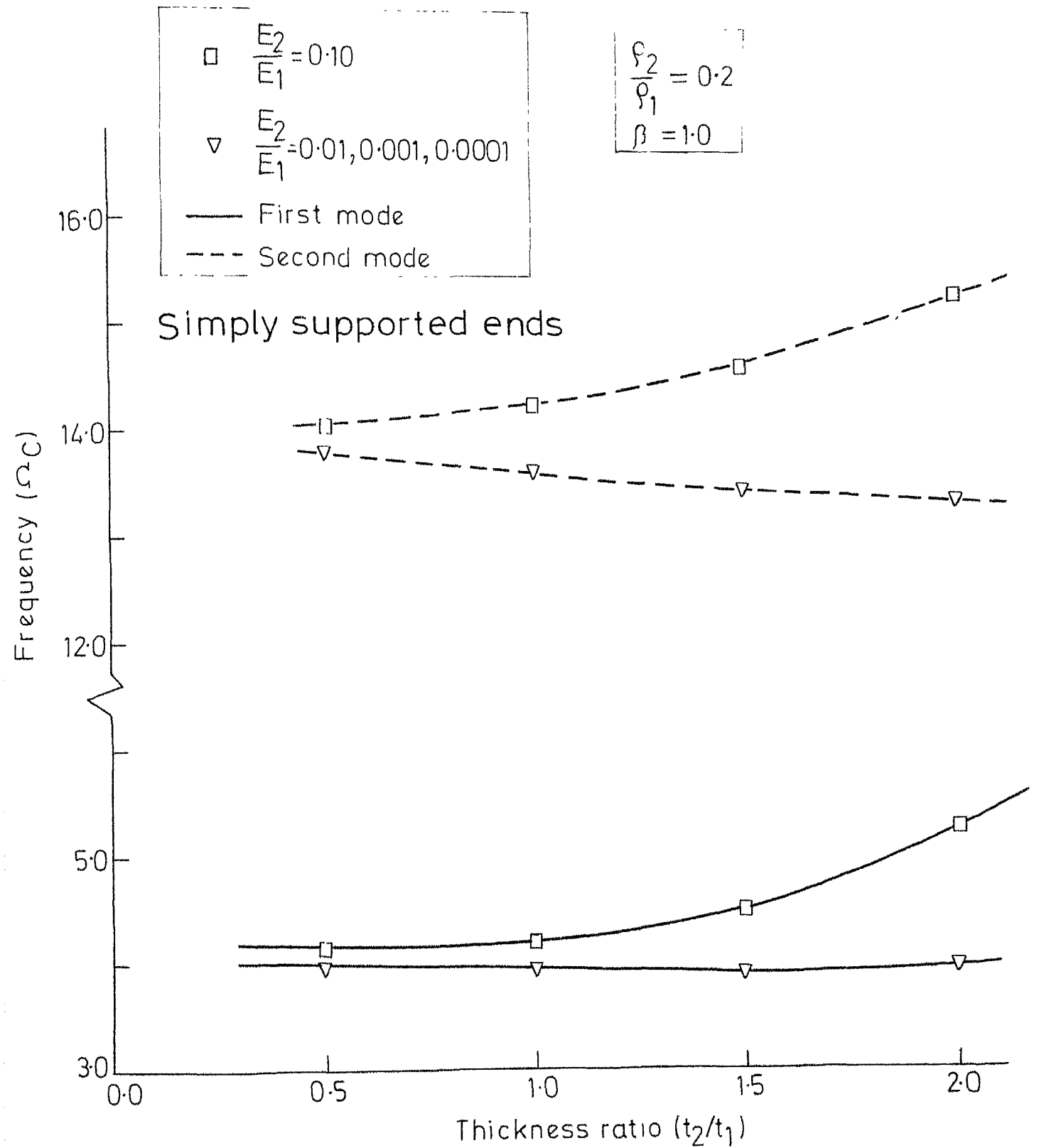
Fig. 4.13 Variation of natural frequency with thickness ratio
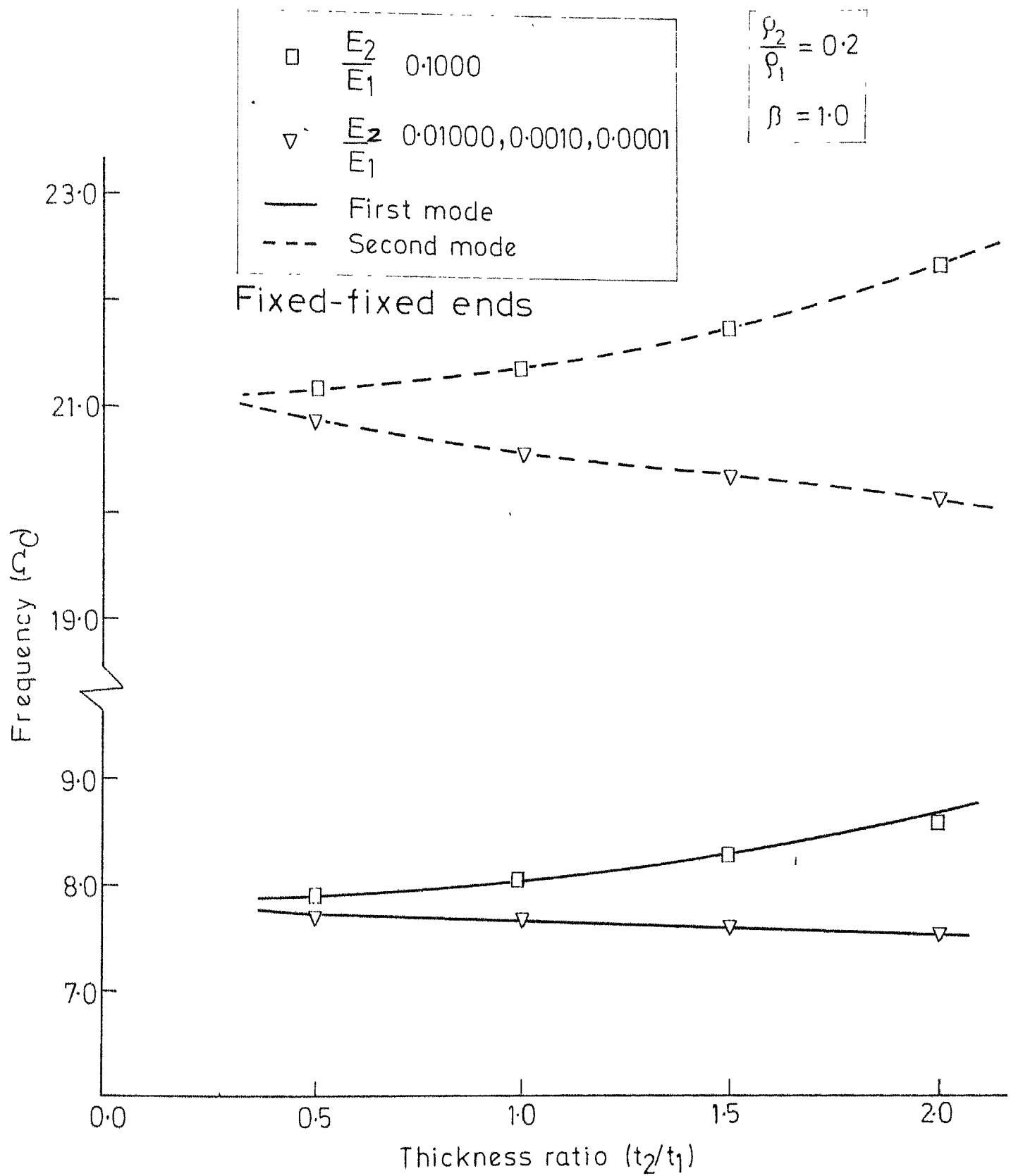
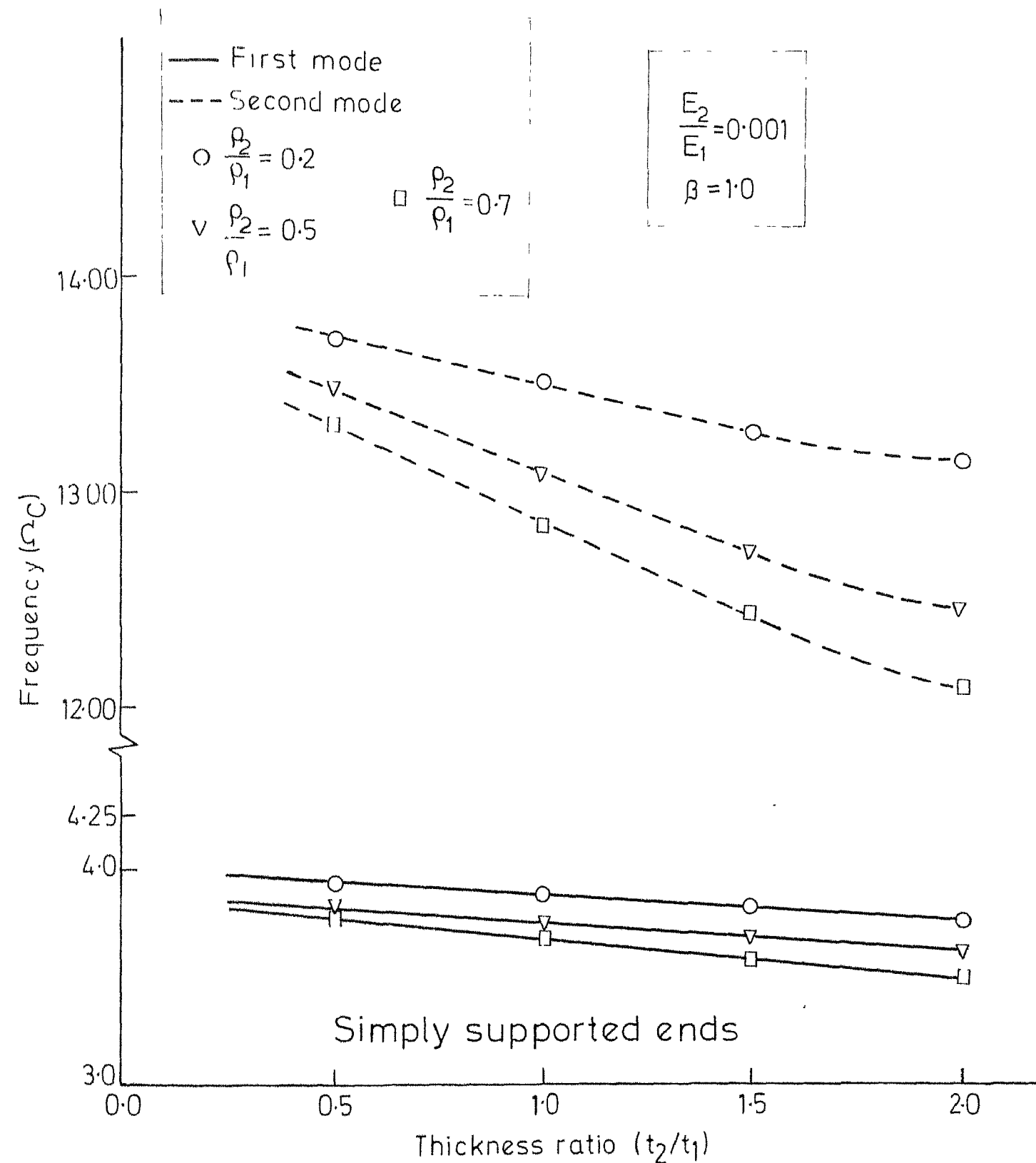Fig. 4.14 Variation of natural frequency with thickness ratio

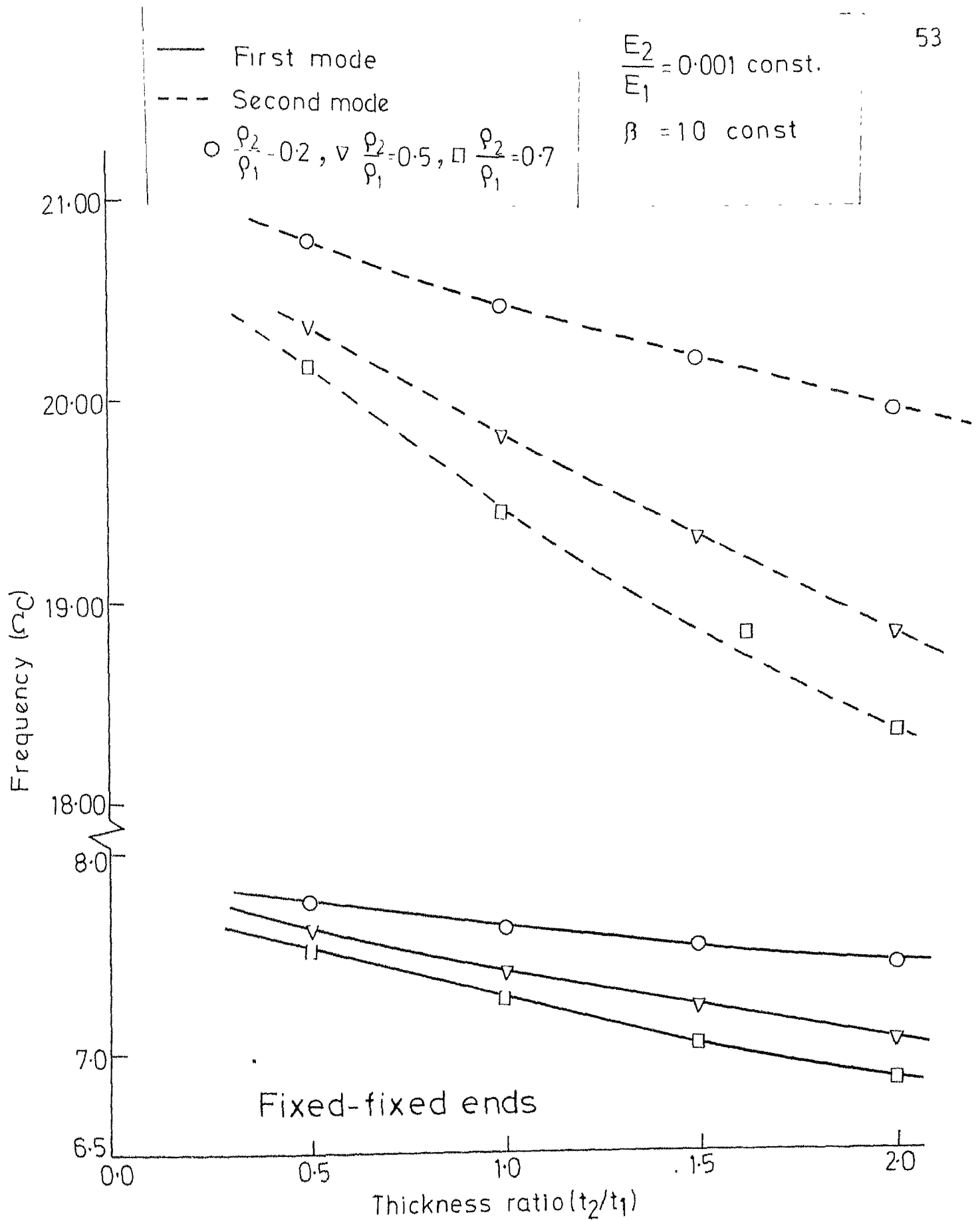Fig. 4·15 Variation of natural frequency with thickness ratio

Fig.4·16 Variation of natural frequency with thickness ratio

CHAPTER 5

CONCLUSIONS

An analysis for free vibration characteristics of a thin walled open section beam with unconstrained visco-elastic layer at the flanges is presented. Transverse vibrations both in and out of the plane of symmetry are considered. In the later case, the bending and the twisting modes are coupled. The natural frequency and modal loss factors, for both type of vibrations, are reported for various values of the parameters involved.

The nature of variation of the modal loss factor with different parameters are found to be similar in both cases. The important observations include the almost linear variation of the modal loss factor with the ratio of elastic moduli and with the loss factor of the viscoelastic material. However, in the coupled modes, the loss factor even with the unconstrained layer, depends on the end conditions and the modal number. The treatment appears to be more effective in damping out the lower order coupled modes.

REFERENCES

1. Sengupta, G., Methods of Reducing Low Frequency Cabin Noise and Sonically Induced Stresses, Based on the Intrinsic Structural Tuning Concept, Paper Presented at the Eighteenth Structures, Dynamics Specialist Conference of AIAA, San Diego, 1977.

2. Ruzicka, J.E., Structural Damping, Section Three, Pergamon Press, Oxford, 1960.

3. Kerwin, E.M., Damping of Flexural Waves by a Constrained Visco-elastic Layer, Journal of the Accoustical Society of America, Vol. 31, p. 952, 1959.

4. Ross, D., Ungar, E., and Kerwin, E.M., Damping of Plate Flexural Vibrations by Means of Viscoelastic Laminae, Structural Damping, Section Three, Edited by E.J. Ruzicka, Pergamon Press, Oxford, 1960.

5. Ditaranto, R.A., Theory of Vibratory Bending for Elastic and Viscoelastic Layered Finite Length Beams, Journal of Applied Mechanics, Vol. 32, p. 881, 1965.

6. Mead, D.J., and Markus, S., The Forced Vibration of a Three Layer, Damped Sandwich Beam with Arbitrary Boundary Conditions, Journal of Sound and Vibration, Vol. 10, p. 163, 1969.

7. Mead, D.J., and Markus, S., Loss Factor and Resonant Frequencies of Encastre Damped Sandwich Beams, Journal of Sound and Vibration, Vol. 12, p. 99, 1970.

8. Mead, D.J., The damping Properties of Elastically Supported Sandwich Plates, Journal of Sound and Vibration, Vol. 24, p. 275, 1972.

9. Mead, D.J., Loss Factors and Resonant Frequencies of Periodic Damped Sandwich Plates, Transactions of the ASME, Journal of Engineering for Industry, Paper No. 75-DET-19, 1975.

10. Gere, J.M. and Lin, Y.K., Coupled Vibration of Thin Walled Beams of Open Cross Section, Journal of Applied Mechanics, Vol. 25, p. 373, 1958.

11. Sengupta, G., and Small, E.F., Experiments on Damping Hat Section Stringers with Constrained Viscoelastic Layers, Boeing Document No. D6 - 42331, 1976.

12. Lin, Y.K., Dynamic Characteristics of Continuous Skin-Stringer Panels, Accoustical Fatigue in Aerospace Structures, Edited by W.J. Trapp and D.M. Forney, Syracuse University Press, p. 163, 1965.

13. Gere, J.M., Torsional Vibrations of Beams of Thin Walled Open Section, Journal of Applied Mechanics, Vol. 21, p. 381, 1954.

14. Seely, F.B., and Smith, O.J., Resistance of Materials, N.Y. Wiley, 1956.

15. Seely, F.B., and Smith, O.J., Advance Mechanics of Materials, N.Y. Wiley, 1959.

16. Timoshenko, S.P., and Goodier, N.J., Theory of Elasticity, Chapter Ten, McGraw Hill Kogakusha Limited, Tokyo, 1970.

17. Timoshenko, S.P., and Gere, J.M., Theory of Elastic Stability, Chapter Five, McGraw Hill Book Company Inc., London, 1961.

18. Johnson, A.F., and Woolf, A., Dynamic Torsion of Two Layer Viscoelastic Beam, Journal of Sound and Vibration, Vol. 48, p. 251, 1976.

19. Carnhan, B., Luther, H.A., and Wilkes, J., Applied Numerical Methods, John Wiley and Sons, Inc., New York, 1969.

20. Sengupta, G., Reduction of Low Frequency Cabin Noise During Cruise Conditions by Stringer and Frame Damping, AIAA Ninteenth Structural Dynamics Conference, Bethesda, Maryland, 1978.

APPENDIX A

DETAILS FOR THIN WALLED OPEN SECTION

A-1 Section Properties

Various dimensions of the cross section are shown in Figure A-1 where O is the shear centre and C is the centroid.

(i)   Area $A = 2 l_1 t_1 + l_2 t_1 + 2 h t_1$

(ii) Centroid position, $\bar{\zeta} = \{ (l_2 t_1^2 + 2 h^2 t_1$

$$+ 2 l_1 t_1 (2 h + t_1) \} / 2A$$

(iii) Area moment of inertia about η axis,

$$I_\eta = \frac{l_2 t_1^3}{3} + \frac{2}{3} h^3 t_1 + \frac{2}{3} l_1 t_1^3 + 2 l_1 t_1 h (h + t_1)$$
$$- A \bar{\zeta}^2$$

(iv) Area moment of inertia about ζ axis

$$I_\zeta = \frac{t_1 l_2^3}{12} + \frac{1}{6} t_1 l_1^3 + \frac{l_1 t_1}{2} (l_1 + l_2)^2 + \frac{1}{6} h t_1^3$$
$$+ \frac{h t_1}{2} l_2^2$$

(v)   Saint Venant's torsion constant

$$C_s = \frac{2}{3} l_1 t_1^3 + \frac{2}{3} h t_1^3 + \frac{1}{3} l_2 t_1^3$$

(vi) Location of shear centre

$$e = \frac{t_1 l_2}{I_\zeta} \left(\frac{l_1 l_2 h}{2} + \frac{l_1^2 h}{2} + \frac{l_2 h^2}{4} \right)$$
$$- \frac{2 t_1 h l_1^2}{I_\zeta} \left(\frac{l_2}{4} + \frac{l_1}{3} \right)$$
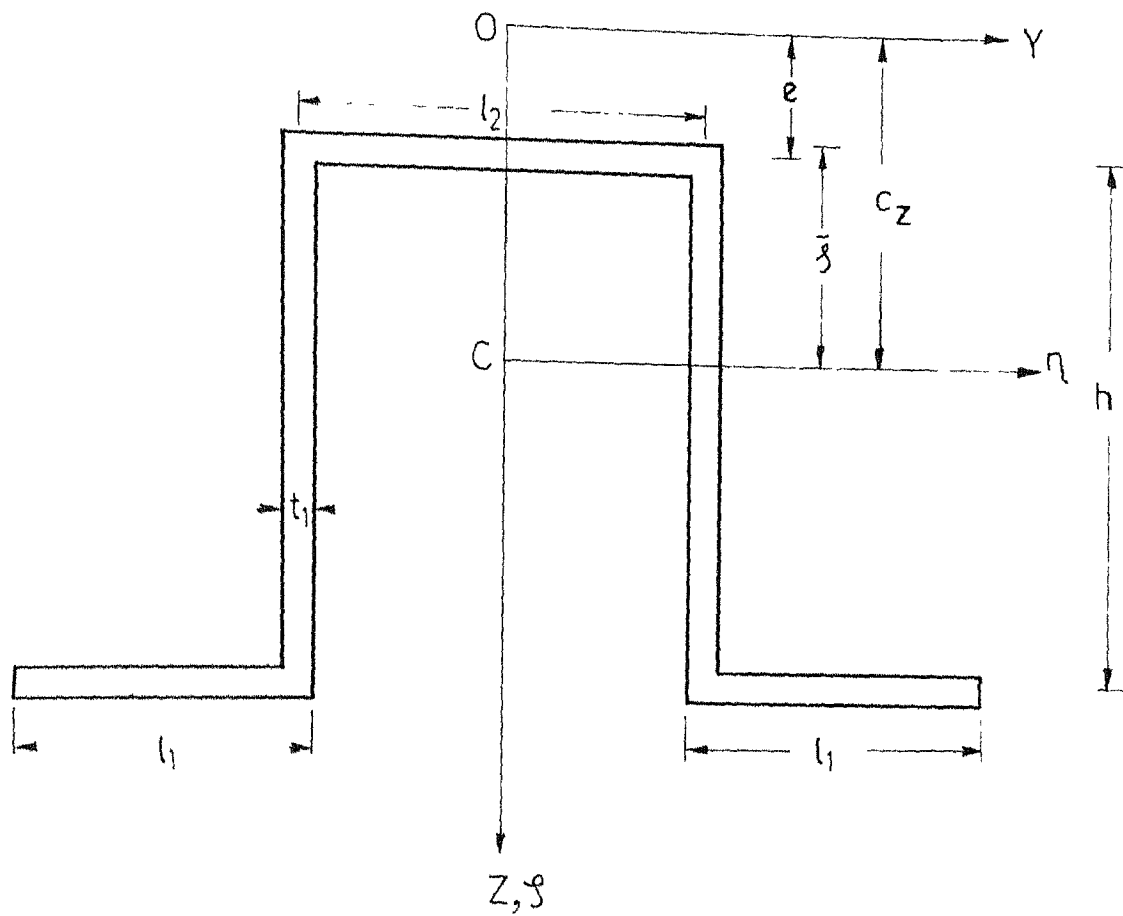
Fig.A-1 A typical top hat section with various dimensions

(vii) $\quad c_z = e + \bar{\zeta}$

(viii) Warping constant

$$C_w = t_1 \{ I_1 + I_2 + I_3 + I_4 + I_5 - m \bar{w}_s^2 \}$$

where $\quad m = 2 l_1 + l_2 + 2 h$

$$\bar{w}_s = \frac{l_2 h}{2} - l_1 (h + e) - \frac{e l_2}{2}$$

$$I_1 = (h + e)^2 l_1^3 / 3$$

$$I_2 = \frac{h}{12} \{ 12 l_1^2 (h + e)^2 + h^2 l_2^2$$

$$- 6 h l_1 l_2 (h + e) \}$$

$$I_3 = \frac{l_2}{12} \{ 3 a^2 + 4 e^2 l_2^2 - 6 l_2 e a \}$$

where $\quad a = l_2 h - 2 l_1 (h + e)$

$$I_4 = \frac{h}{12} \{ 3 b^2 + 3 h l_2 b + h^2 l_2^2 \}$$

where $\quad b = l_2 h - 2 l_1 (h + e) - 2 e l_2$

$$I_5 = \frac{l_1}{3} \{ 3 d^2 + (h + e)^2 l_1^2 + 3 l_1 (h + e) d \}$$

where $\quad d = l_1 (h + e) + e l_2 - h l_2$

A-2 Non Dimensional Terms in Equation (2.6)

$$\alpha_1 = - g_1' \, l^2$$
$$\alpha_2 = - (1 + p_1' + s_1')$$
$$\alpha_3 = g_1' \, l^2$$
and $\alpha_4 = s_1'$

where $\quad g_1' = \dfrac{G}{E}\dfrac{C_S}{C_W}$

$$p_1' = \dfrac{I_\zeta}{C_W}\,c_z^2$$

$$s_1' = \dfrac{I_C}{C_W} \times \dfrac{I_\zeta}{A}$$

1 is the length of the beam.

Non dimensional natural frequency

$$\Omega_n^2 = \dfrac{\omega^2}{\dfrac{E\,I_\zeta}{\rho A\,1^4}}$$

where ω is the natural frequency.

A.3 Appropriate Boundary Conditions for the Coupled Vibration

For simply supported ends the boundary conditions are

$$v_o = 0$$
$$v_o^{ii} = 0$$
$$\psi = 0 \quad \text{or} \quad v_o^{iv} = 0$$
and $\quad \psi^{ii} = 0 \quad \text{or} \quad v_o^{vi} = 0$

at $x = 0$
and $x = 1$

For fixed - fixed ends, the boundary conditions are

$$v_o = 0$$
$$v_o^{i} = 0$$
$$\psi = 0 \quad \text{or} \quad v_o^{iv} = 0$$
$$\psi^{i} = 0 \quad \text{or} \quad v_o^{v} = 0$$

at $x = 0$
and $x = 1$

A.4   Elements of Matrix A in Equation (2.8)

Elements of the matrix A is different for different boundary conditions. For simply supported ends:

$$[A] = \begin{bmatrix} 1.0 & 1.0 & 1.0 & \cdots & \cdots & 1.0 \\ e^{\lambda_1} & e^{\lambda_2} & e^{\lambda_3} & \cdots & \cdots & e^{\lambda_8} \\ \lambda_1^2 & \lambda_2^2 & \lambda_3^2 & \cdots & \cdots & \lambda_8^2 \\ \lambda_1^2 e^{\lambda_1} & \lambda_2^2 e^{\lambda_2} & \lambda_3^2 e^{\lambda_3} & \cdots & \cdots & \lambda_8^2 e^{\lambda_8} \\ \lambda_1^4 & \lambda_2^4 & \lambda_3^4 & \cdots & \cdots & \lambda_8^4 \\ \lambda_1^4 e^{\lambda_1} & \lambda_2^4 e^{\lambda_2} & \lambda_3^4 e^{\lambda_3} & \cdots & \cdots & \lambda_8^4 e^{\lambda_8} \\ \lambda_1^6 & \lambda_2^6 & \lambda_3^6 & \cdots & \cdots & \lambda_8^6 \\ \lambda_1^6 e^{\lambda_1} & \lambda_2^6 e^{\lambda_2} & \lambda_3^6 e^{\lambda_3} & \cdots & \cdots & \lambda_8^6 e^{\lambda_8} \end{bmatrix}$$

Here, λ_1, λ_2, ... λ_8 are eight roots of the characteristic polynomial equation (2.7).

For fixed ends beam:

$$[A] = \begin{bmatrix}
1.0 & 1.0 & 1.0 & \cdots & \cdots & 1.0 \\
e^{\lambda_1} & e^{\lambda_2} & e^{\lambda_3} & \cdots & \cdots & e^{\lambda_8} \\
\lambda_1 & \lambda_2 & \lambda_3 & \cdots & \cdots & \lambda_8 \\
\lambda_1 e^{\lambda_1} & \lambda_2 e^{\lambda_2} & \lambda_3 e^{\lambda_3} & \cdots & \cdots & \lambda_8 e^{\lambda_8} \\
\lambda_1^4 & \lambda_2^4 & \lambda_3^4 & \cdots & \cdots & \lambda_8^4 \\
\lambda_1^4 e^{\lambda_1} & \lambda_2^4 e^{\lambda_2} & \lambda_3^4 e^{\lambda_3} & \cdots & \cdots & \lambda_8^4 e^{\lambda_8} \\
\lambda_1^5 & \lambda_2^5 & \lambda_3^5 & \cdots & \cdots & \lambda_8^5 \\
\lambda_1^5 e^{\lambda_1} & \lambda_2^5 e^{\lambda_2} & \lambda_3^5 e^{\lambda_3} & \cdots & \cdots & \lambda_8^5 e^{\lambda_8}
\end{bmatrix}$$

APPENDIX B

GEOMETRIC AND ELASTIC PROPERTIES FOR COMPOSITE CROSS SECTION

B.1 Section Properties

Figure B.1 shows the composite cross section where $\eta_1 - \eta_1$ and $\eta_2 - \eta_2$ are the centroidal axis of parts 1 and 2 respectively. C is the mass centre of the composite section.

$$\bar{\zeta}_c = \frac{A_1 \, \rho_1 \, \bar{\zeta}_1 + A_2 \, \rho_2 \, \bar{\zeta}_2}{A_1 \, \rho_1 + A_2 \, \rho_2}$$

where $A_1, \bar{\zeta}_1$ are given as A and $\bar{\zeta}$ respectively in Appendix A. ρ_1 and ρ_2 are the mass densities of the material of 1 and 2 respectively.

$$A_2 = 2 \, l_1 \, t_2, \quad \bar{\zeta}_2 = (h + t_1 + \frac{t_2}{2})$$

$$I_{\zeta_1} = I_\zeta \quad \text{given in Appendix A.}$$

$$I_{\zeta_2} = \frac{1}{6} \, t_2 \, l_1^3 + \frac{t_2 \, l_1}{2} \, (l_1 + l_2)^2$$

where I_{ζ_1} and I_{ζ_2} are the area moments of inertia of part 1 and 2 about the axis of symmetry .

B.2 Shear Centre Location for Composite Beam
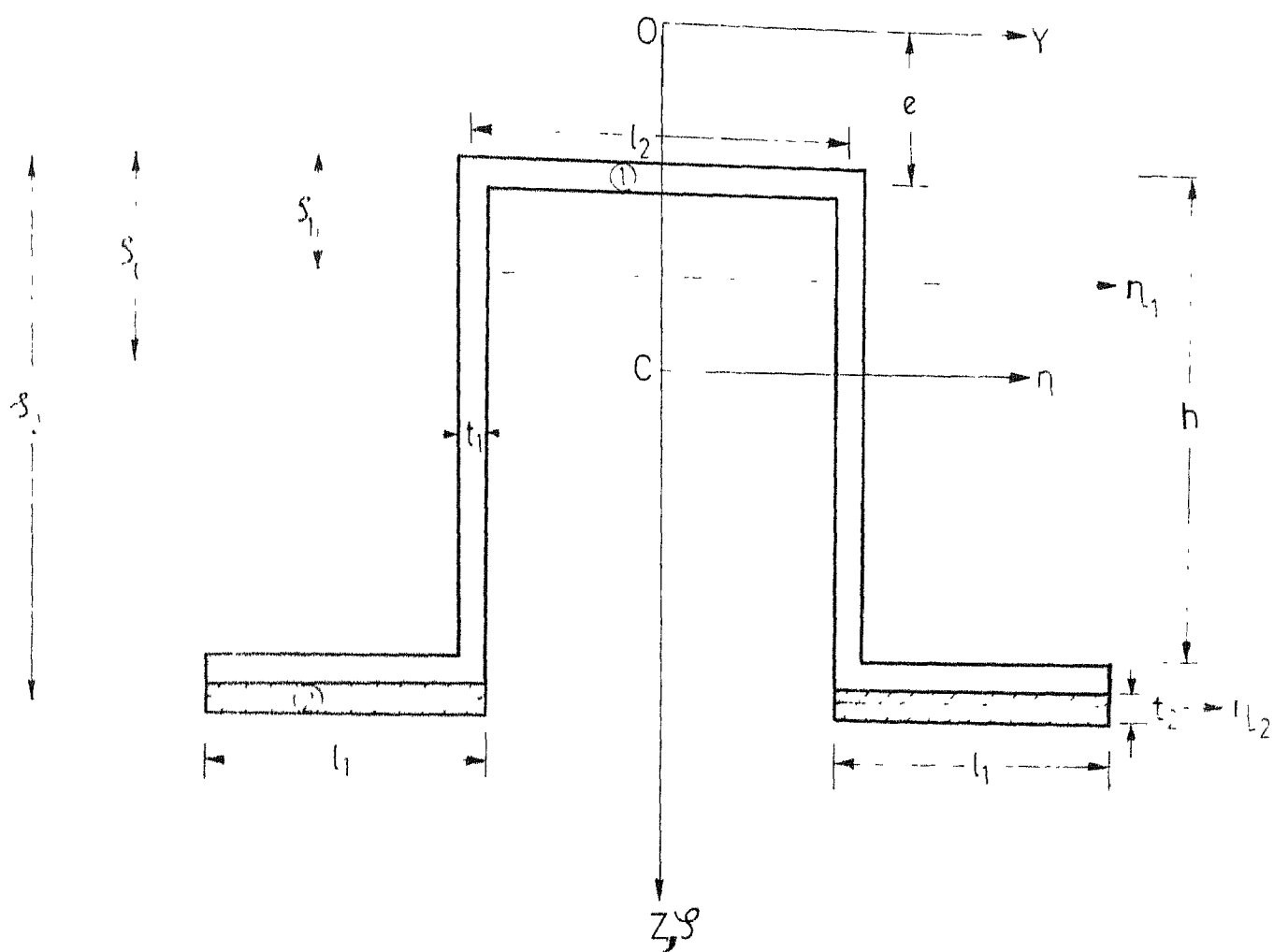
$$e = V_3 \, l_2 - V_1 \, (2h + t_1 + t_2) - 2 \, V_2 \, h$$

Fig. B-1 Composite cross section with the damping layer

$$V_3 = \frac{E_1}{4} \frac{\{ 2\, l_1\, h\, (l_1 + l_2)\, t_1 + t_1\, l_2\, h^2 \}}{(E_1\, I_{\zeta_1} + E_2^*\, I_{\zeta_2})}$$

$$V_2 = \frac{t_1\, E_1}{(E_1\, I_{\zeta_1} + E_2^*\, I_{\zeta_2})}\, l_1^2\, \left(\frac{l_2}{4} + \frac{l_1}{3} \right)$$

$$\text{and} \quad V_1 = \frac{t_2\, E_2^*}{(E_1\, I_{\zeta_1} + E_2^*\, I_{\zeta_2})}\, l_1^2\, \left(\frac{l_2}{4} + \frac{l_1}{3} \right)$$

with $E_2^* = E_2\,(1 + i\,\beta)$; $\beta = $ loss factor of the

viscoelastic material.

B.3 Torsional Rigidity of the Composite Beam

$$C_1 = 4\, l_1\, G_1\, \left(\frac{2}{3} t_1^3 + \frac{1}{2} \mu\, t_1^2 \right)$$

$$+ 4\, l_1\, G_2^*\, \left(\frac{2}{3} t_2^3 - \frac{1}{2} \mu\, t_2^2 \right)$$

$$+ G_1\, \left(\frac{2}{3} h + \frac{1}{3} l_2 \right) t_1^3$$

$$\text{where} \quad \mu = \frac{G_2^*\, t_2^2 - G_1\, t_1^2}{G_2^*\, t_2 + G_1\, t_1}$$

with $G_2^* = G_2\,(1 + i\,\beta)$

B.4 Warping Rigidity of the Composite Beam

$$C_2 = E_1\, t_1\, C_{w_1} + E_2^*\, t_2\, C_{w_2}$$

where C_{w_1} = warping constant of cross section 1

as C_w in Appendix A .

$$C_{W_2} = \frac{(h + e + t)^2 \, 1_1^3}{6}$$

where $t = \left(\frac{t_1 + t_2}{2} \right)$

APPENDIX C

DETAILS FOR THE FREE VIBRATION OF COMPOSITE
BEAM IN COUPLED MODE

C.1 Section Properties

The various section properties can be written for the composite cross section shown in Figure B-1, as

$$I_{\eta_1} = I_\eta + A_1 \left(\bar{\zeta}_c - \bar{\zeta}_1 \right)^2$$

$$I_{\eta_2} = \frac{l_1 t_2^3}{6} + A_2 \left(\bar{\zeta}_c - \bar{\zeta}_2 \right)^2$$

$$I_{c_1} = I_{\eta_1} + I_{\zeta_1}$$
$$I_{c_2} = I_{\eta_2} + I_{\zeta_2}$$

where I_η, I_{ζ_1}, I_{ζ_2}, $\bar{\zeta}_1$, $\bar{\zeta}_c$, $\bar{\zeta}_2$ etc. are given in previous appendices.

C.2 Non Dimensional Terms in Equation (4.18)

$$\alpha_1 = - g\, l^2$$
$$\alpha_2 = - (q + p + s)$$
$$\alpha_3 = g\, q\, l^2$$
$$\alpha_4 = s\, q$$

where

$$g = \frac{C_1}{C_2}$$

C_1 and C_2 are the torsional and the warping rigidity given in Appendix B .

$$q = \left(-\frac{\rho_1 A_1 + \rho_2 A_2}{E_1 I_{\zeta_1} + E_2^* I_{\zeta_2}} \right) \times \left(\frac{E_1 I_{\zeta_1} + E_2 I_{\zeta_2}}{\rho_1 A_1 + \rho_2 A_2} \right)$$

where E_2 is the real part of E_2^*.

$$p = \left(\frac{\rho_1 A_1 + \rho_2 A_2}{C_2} c_z^2 \right) \times \left(\frac{E_1 I_{\zeta_1} + E_2 I_{\zeta_2}}{\rho_1 A_1 + \rho_2 A_2} \right)$$

$$s = \left(\frac{\rho_1 I_{c_1} + \rho_2 I_{c_2}}{C_2} \right) \times \left(\frac{E_1 I_{\zeta_1} + E_2 I_{\zeta_2}}{\rho_1 A_1 + \rho_2 A_2} \right)$$

Non dimensional natural frequency is given by

$$\Omega_c^2 (1 + i \nu) = \frac{\omega^2 (1 + i \eta)}{\dfrac{E_1 I_{\zeta_1} + E_2 I_{\zeta_2}}{(\rho_1 A_1 + \rho_2 A_2) l^4}}$$

where ω is the natural frequency

Ω_c is the nondimensional natural frequency

and η is the composite loss factor.

$\nu = \eta$.

C.3 Elements of Matrix A in Equation (4.20)

The form of matrix A is same as given in Appendix A.4. Here, λ_1, λ_2 ... are the eighth root of characteristic polynomial equation given in Equation (4.19).